ADVANCED HEALTHCARE MATERIALS
www.advhealthmat.de

# Electroconductive Nanocellulose, a Versatile Hydrogel Platform: From Preparation to Biomedical Engineering Applications

*Myoung Joon Jeon, Aayushi Randhawa, Hojin Kim, Sayan Deb Dutta, Keya Ganguly, Tejal V. Patil, Jieun Lee, Rumi Acharya, Hyeonseo Park, Youjin Seol, and Ki-Taek Lim**

**Nanocelluloses have garnered significant attention recently in the attempt to create sustainable, improved functional materials. Nanocellulose possesses wide varieties, including rod-shaped crystalline cellulose nanocrystals and elongated cellulose nanofibers, also known as microfibrillated cellulose. In recent times, nanocellulose has sparked research into a wide range of biomedical applications, which vary from developing 3D printed hydrogel to preparing structures with tunable characteristics. Owing to its multifunctional properties, different categories of nanocellulose, such as cellulose nanocrystals, cellulose nanofibers, and bacterial nanocellulose, as well as their unique properties are discussed here. Here, different methods of nanocellulose-based hydrogel preparation are covered, which include 3D printing and crosslinking methods. Subsequently, advanced nanocellulose-hydrogels addressing conductivity, shape memory, adhesion, and structural color are highlighted. Finally, the application of nanocellulose-based hydrogel in biomedical applications is explored here. In summary, numerous perspectives on novel approaches based on nanocellulose-based research are presented here.**

## 1. Introduction

Natural hydrophilic polymer-based hydrogels can be appropriately designed and functionally tuned for different biomedical operations.[1] Hydrogel is a 3D crosslinked network of hydrophilic polymer, which chains through physical interaction (hydrogen bonding,[2] ionic bonding[3]) or chemical (covalent bonding[4]). Several natural hydrophilic polymers, such as polysaccharides,[5] proteins,[6] and DNA,[7] can form these networks to synthesize hydrogels that maintain significant amounts of interstitial water. Because of their great biocompatibility, these hydrogels are suitable for a wide range of biomedical applications. Nonetheless, they have evident disadvantages, such as inadequate mechanical qualities, difficulties in managing their degradation and structure due to their synthesis technique, and possible immunogenicity, which restricts their use for more widespread purposes.[8]

Cellulose has been introduced commonly for hydrogels due to its high accessibility and efficiency in improving mechanical hardness, together with its biodegradability, sustainability, and biocompatibility.[9] Cellulose is a natural polymer that is found in plants with cell walls and the monomer of a cellulose chain is $\beta$-d-glucose linked through a $\beta$-1,4-glucoside bond, chemical formula $(C_6H_{10}O_5)_n$. Cellulose has a relatively straightforward chain structure of repeating elements with several hydroxyl groups on glucose rings forming hydrogen bonds. These chain structures have high crystallinity, so they show tensile strength ($\sigma$) of 2–7.7 GPa, crystalline elastic modulus ($E$) $\approx$ 140 GPa, and density ($\rho$) $\approx$ 1.6 g cm$^{-3}$. These properties provide a strength that is seven times higher than steel while also being lightweight and having excellent characteristics, including low thermal expansion (**Table 1**). Also, its properties show better mechanical performance and stability than other similar natural polymers.[10] When cellulose is broken down into nanosized units, it can produce nanocellulose. Nanocellulose is classified into cellulose nanocrystals (CNCs) with excellent crystallinity and strength,[11] cellulose nanofibers (CNFs) with superior flexibility and mechanical properties,[12] bacterial nanocelluloses (BNCs) with outstanding moisture and gas regulation capabilities,[13] etc., depending on the fiber morphology, crystallinity, and chemical treatment.[14] The crystalline region of nanocellulose-based hydrogels, formed by high crystallinity

M. J. Jeon, A. Randhawa, H. Kim, S. D. Dutta, K. Ganguly, T. V. Patil, J. Lee, R. Acharya, H. Park, Y. Seol, K.-T. Lim
Department of Biosystems Engineering
Kangwon National University
Chuncheon 24341, Republic of Korea
E-mail: ktlim@kangwon.ac.kr
M. J. Jeon, A. Randhawa, H. Kim, T. V. Patil, J. Lee, R. Acharya, H. Park, Y. Seol, K.-T. Lim
Interdisciplinary Program in Smart Agriculture
Kangwon National University
Chuncheon 24341, Republic of Korea
S. D. Dutta, K. Ganguly, K.-T. Lim
Institute of Forest Science
Kangwon National University
Chuncheon 24341, Republic of Korea
The ORCID identification number(s) for the author(s) of this article can be found under https://doi.org/10.1002/adhm.202403983

**DOI: 10.1002/adhm.202403983**

 

**Table 1.** Properties of nanocellulose compared to various other reinforcing materials. Adapted with permission. Copyright 2021, Wiley-VCH.[19]

| Material | $\rho$ [g cm$^{-3}$] | $\sigma$ [GPa] | $E$ [GPa] | CTE[a] [ppm K$^{-1}$] | Refs. |
|---|---|---|---|---|---|
| Kevlar-49 fiber | 1.4 | 3.6–4.1 | 127–131 | −2.0 | [20] |
| Carbon fiber | 1.8 | 1.5–5.5 | 150–500 | −0.6 | [20] |
| Mild steel | – | 0.4–0.6 | 194–243 | – | [21] |
| High strength steel | – | 0.8–0.9 | 207–242 | – | [21] |
| Stainless steel | 7.8 | 0.4–1.8 | 193–204 | 10.2–17.2 | [20] |
| Clay nanoplatelets | – | – | 170 | – | [22] |
| Carbon nanotubes (CNTs) | – | 11–63 | 270–950 | – | [23] |
| Nanochitin | 1.6 | 1.6–3 | 41–70[b] | 21 | [24] |
| Nanocellulose | 1.6 | 2–7.7 | ≈140[b] | 0.1[c], 6[d] | [25] |

[a] CTE, coefficient of thermal expansion [b] $E$ of the crystalline region [c] CTE of the all-cellulose composite measured using a thermomechanical analyzer [d] CTE of the crystalline region measured by X-ray diffraction.

and hydrogen bonding, can block external gases[15] and regulate drug release by stimulation.[16] Nanocellose-based hydrogels with rheological properties can contract and relax in response to activity-induced changes without being destroyed, thereby also serving as sensors.[17] Because of the reversible and irreversible interactions between the nanocellulose and polymeric backbones, nanocellulose-based hydrogels exhibit intriguing rheological characteristics while maintaining good mechanical properties, serving as reinforcing agents for 3D printing.[11] The tunable viscosity and shear peeling behavior of nanocellulose-based hydrogels facilitate precise extrusion and layer-by-layer deposition in the 3D printing process, ensuring high resolution and structural fidelity to the print.[18]

Natural polymers' cell-signaling and cell-interactive properties might be combined with electrical stimulation and applied to neuronal, muscular, and cutaneous tissue engineering applications. Accordingly, imparting conductivity to hydrogels expands their applications in biosensing[26] or promotes tissue regeneration by stimulating endogenous electrical fields.[27] Due to the tunable conductivity and mechanical properties of nanocellulose-based conductive hydrogels, this kind of hydrogel has a high potential for multifunctional application.[28] Hydrogels' electronic and ionic transport could be enhanced when they are fabricated into materials with a high surface area and a porous structure.[29] Electroconductive hydrogels' mechanical properties may be adjusted utilizing a variety of synthetic techniques and technologies, thus broadening their applicability. Their improved biocompatibility reduces the toxicity of the electroactive materials, allowing them to be exposed to the natural environment of the human body.

This review sheds light on nanocellulose-based research in the biomedical field. The review discusses different types of nanocellulose and their extraction methods. Next, the advancement in nanocellulose-based hydrogels and their preparation methods, using 3D printing methods, are also highlighted. The review presents an overview of the methods to develop nanocellulose-based conductive hydrogels based on the use of conductive polymers, including carbon nanomaterials and carbon dots. Additionally, the development of shape-memory, tunable, and structural color based on nanocellulose research has also been explored. Finally, the review summarizes the limitations and future opportunities for the advancement of nanocellulose-based research. **Scheme 1** depicts the overview of the current review paper.

## 2. Nanocellulose and Its Types

Plant cell walls are made up of semi-crystalline microfibrils of cellulose embedded in an amorphous lignin and hemicellulose matrix.[17] The desirable alignment of cellulose crystals can be a crucial determinant of the mechanical properties of the cell wall and the interactions between cellulose-cellulose and cellulose-matrix[34] (**Figure 1a**). Nanocellulose acquires functions of charge transport because its structure implies a large surface area and unique properties. The cellulose surface possesses numerous hydroxyl groups (—OH), which can be further utilized as a substrate for various modifications, i.e., aldehyde, carboxylic acid, and amine groups, as described in **Table 2**. The three different types of nanocellulose, namely CNCs, BNCs, and CNFs, are categorized based on the type of their extraction methods.

In the BNCs, surface modifications occur during the manufacturing process depending on the bacterial strain and cultivation conditions (Figure 1b). Additives are introduced to improve and impart additional characteristics such as biocompatibility and interaction with proteins. These chemical modifications can impart either positive or negative electrical charges, resulting in electrical, optical, or other stimulus-responsive characteristics.[47]

### 2.1. CNCs

CNCs are the most extensively researched type of nanocellulose, with polymer chains typically ranging from 100 to 500 nm in length. Both inorganic acid hydrolysis and enzymatic processes are employed to extract CNCs from cellulose fibers.[48] CNCs production primarily involves chemical treatment to swell the amorphous regions while maintaining the surface crystalline portion.[48] A commonly used method involves sulfuric acid. Sulfate groups anchor themselves to the CNCs surface through esterification and this causes repulsive negative charges on the compound's surface and high colloidal stability.[49] Besides, it structurally preserves cellulose's heat stability and gives rise to highly crystalline rod-like nanostructures from the amorphous zones.[50] Adjusting the groups attached to the surface is possible depending on the duration of acid hydrolysis during manufacturing.[51] Enzymatic processes offer the potential for coproduction with biofuels and influence the yield and characteristics of nanocellulose-based on various enzymatic hydrolysis properties.[52] CNCs undergo extensive evaluation concerning colloidal stability, size, crystallinity, and thermal stability during production.[53] CNCs exhibit insulating properties due to intramolecular hydrogen bonding, polarity, and hydrophilic surface characteristics, making them challenging for broad applications. Accordingly, surface modification techniques and mechanical processes are being attempted for various commercial and wide-ranging applications.[54] Furthermore, CNCs have many other advantages, including high efficiency, high aspect ratio, low density, and renewable and nontoxic properties, which make CNCs

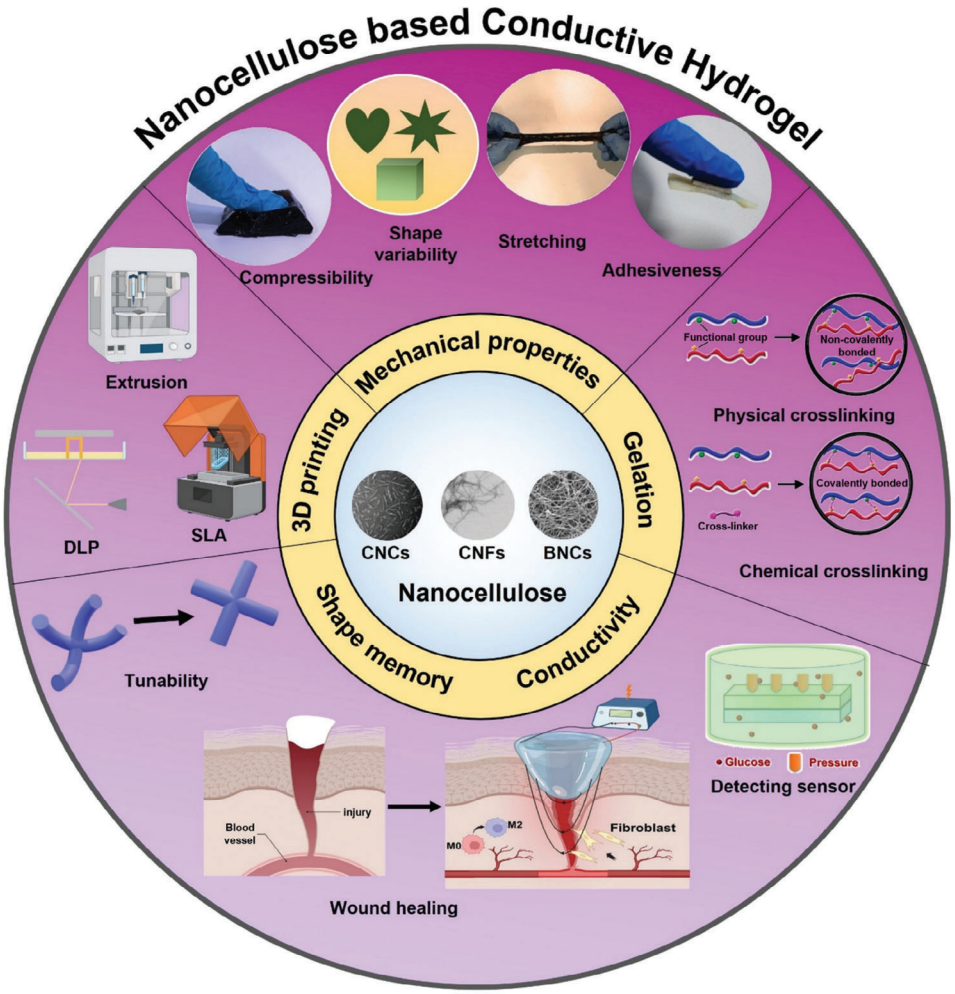


**Scheme 1.** A schematic illustration of the current study. Nanocellulose and its types[30] and its significance in various applications. Nanocellulose-based hydrogels can be fabricated with tunable mechanical properties,[31] gelation,[32] conductivity,[33] shape memory, and 3D printing. Copyright 2020, The Authors, published by MDPI; Copyright 2022, Elsevier Ltd; Copyright 2019, Nature Publishing Group; Copyright 2021, Elsevier Ltd.

ideal templates with various compound properties and synergistic effects under diverse conditions.[55] For instance, hydrogels synthesized and developed through CNCs provide a desirable drug-releasing channel in the hydrogel network as well as favorable attributes for wound healing applications, including low cytotoxicity, high swelling properties, and biocompatibility.[56]

### 2.2. CNFs

Also known as nanofibrillated cellulose, CNFs refer to bundles of fibers with diameters in the nanometer range and lengths in the micrometer range. CNFs are manufactured into flexible fibril forms through mechanical methods,[57] as well as chemical[44] or biological[58] pretreatment for cellulose fibrillation.[59] The reason for pretreatment in the production of nanofibers is to ensure that during mechanical processing, CNFs can efficiently break down fiber structures, leading to overall homogenization of energy efficiency and final product uniformity.[60] Representatively, CNFs can be produced via the (2,2,6,6,-tetramethyl piperidine-1-yl) oxidanyl (TEMPO) mediated oxidation reaction.[61] The oxidation catalyst utilizing the soluble and nitroxyl radical TEMPO can efficiently modify the surface by transforming alcoholic hydroxyls into carboxylate groups[62] and aldehyde groups,[63] enabling effective surface modification.[64] With high aspect ratios, CNFs exhibit high chemical stability and utilize adjustable surface charges for controlling the orientation and anisotropic characteristics of fibers through magnetic[65] and electric fields.[66] CNFs with outstanding mechanical properties can be aligned controllably through magnetic or electric fields, shear force, and mechanical elongation on a macroscopic scale while employing their nanosystem structures.[67] In one study, wet-state cellulose long fibers were produced through wet spinning, and a 5T magnetic field generated by a superconducting DC magnet was applied vertically. An electric field of 50 V $cm^{-1}$ at 100 Hz was applied along the long fibers between two electrode supports (Figure 1c). As a result of the experiment, it was observed that the tensile modulus and strength of the CNFs increased by 84% and 125%, respectively, due to the combined effects of magnetic and electric fields. This indicates that this method produces highly

 

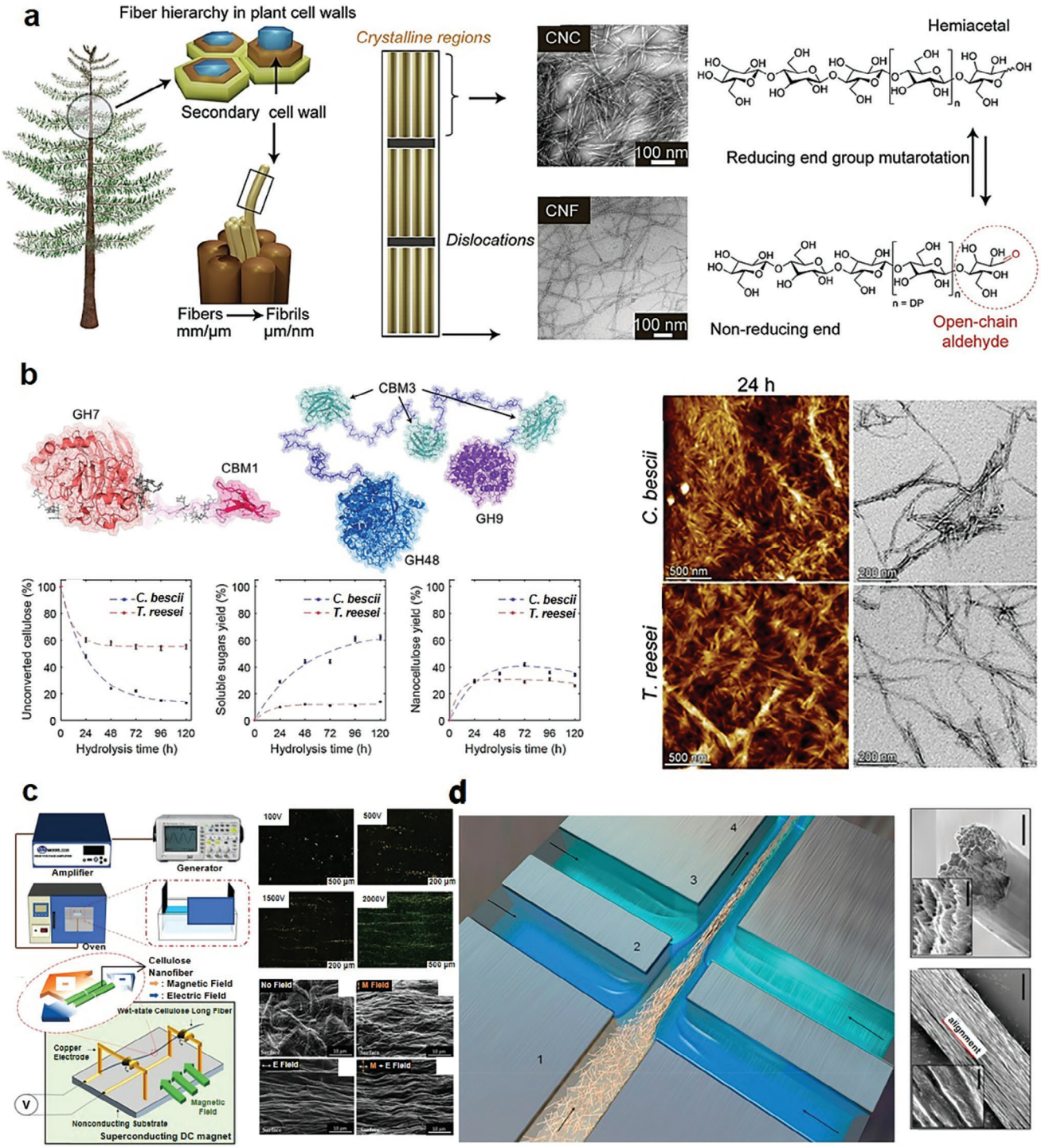


**Figure 1.** a) Schematic diagram of plant cell wall components and images and structures of nanocellulose (CNCs, CNFs).[17] b) Images of BNCs produced by *B. bescii* and *T. reesei*.[52] Copyright 2017, American Chemical Society. c) Alignment experiment of TEMPO-oxidized cellulose nanofibers (TOCNF) by electric and magnetic fields.[65b] Copyright 2019, Springer Nature Link. d) CNFs produced through flow-based assembly.[67a] Copyright 2021, American Chemical Society.

**Table 2.** Types of cellulose surface modification.

| Cellulose type | Method | Surface modification bonding | Application | Ref. |
|---|---|---|---|---|
| CNCs | 3-Aminopropyltriethoxysilane | N—H bending vibration of primary amine | Enhanced thermal stability, high residual carbon formation in high-temperature environments, nano adsorbent | [35] |
| | Alkali (NaOH) treatment | carbonyl carbon (−C =O), methyl carbon ($-CH_3$) | Enhanced crystallization, applicable to a wide range of dispersants | [36] |
| | Acetic anhydride | Acetyl groups (−C=O, C−O−C) | Improved tensile strength, enhancement of the compatibility between poly(3-hydroxybutyrate-co-4-hydroxybutyrate) (PHB) and CNCs | [37] |
| | *n*-Octadecyl isocyanates | Alkyl group | Emulsifying capacity | [38] |
| | Dibutyl tin dilaurate | Isocyanate groups | Increase in tensile strength and fracture work efficiency | [39] |
| | $H_2SO_4/HNO_3$ | Carboxyl group | High degree of crystallinity (thermal stability) | [40] |
| | Triethylamine, acetic anhydride | Carboxyl group | Adjusting drug delivery according to pH by adding paclitaxel | [41] |
| CNFs | $NH_4H_2PO_4$ | Esterification (no weak acid groups) | Extremely high transparency and high viscosity | [42] |
| | Deep eutectic solvents [choline chloride and urea (molar ratio of 1:2)] | Carbamate bond (1715 $cm^{-1}$) | Low toxicity, biodegradable, and exhibit negligible vapor pressure | [43] |
| | Periodate–chlorite oxidation | Carboxyl group | Highly viscous and transparent gel | [44] |
| | Sodium vinyl sulfonate | Sulfonate groups (soft base) | Low susceptibilities to complex and ligand formation with multivalent ions | [45] |
| | Ozone gas, lignin-derived phenolics | Carbonyl groups (1600 $cm^{-1}$) | Tensile and thermal stability, crystallinity, film transparency, turbidity, and water permeability | [46] |

oriented CNFs of enhanced mechanical properties. When a CNF slurry was injected into two intersecting flows, the first flow (with deionized water) guided particle alignment, and the second flow (with an acidic solution) protonated surface carboxyl groups. This led to a reduction of electrostatic repulsion and induced coagulation of the fibers. As the length of the CNFs used in alignment increased, the rotational diffusion time of the particles also increased, leading to higher local order and enhanced mechanical properties (Figure 1d).

### 2.3. BNCs

BNCs are formed by various carbohydrate fermentation induced by microorganisms,[68] especially bacteria,[69] unlike the manufacturing methods of CNCs and CNFs. BNCs are synthesized from glucose through two main stages: the generation of $\beta$-1,4-glucan chains and the crystallization of cellulose.[70] BNCs have promising applications in various fields, but their usage is limited by low production efficiency, which results in increased costs. As a result, research is underway to improve production efficiency through variations in the concentration of raw materials,[71] low-cost production via cellulose-containing byproducts,[72] and investigation of bacteria types used in the fermentation process.[73] BNCs can be adjusted in structure and crystallinity through cultivation conditions,[74] requiring an understanding of the biosynthetic process for new properties and applications. BNCs can be easily manufactured into desired forms, such as tubes or membranes, during the fermentation process, making them readily adaptable to meet the requirements of various application fields.[75] Thus, in comparison with CNCs and CNFs, BNCs have larger aspect ratios, better crystallinity, and the formation of more complex web structures combined with outstanding mechanical characteristics and good chemical stability.[76]

## 3. Methods of Preparation

To create hydrogels from nanocellulose, the nanocellulose hydroxyl groups need to be chemically modified to disperse in a solvent and then crosslinked for gelation to occur. Usually, nanocellulose is dispersed in a solvent by precooling it in alkali/urea aqueous solutions or *N*,*N*-dimethylacetamide/lithium chloride (DMAc/LiCl) to separate cellulose chains or through TEMPO oxidation. Hydroxyl groups are present in a huge amount of cellulose. These groups can interact with other groups to form crosslinking either physically or chemically, and hence, the hydrogels are obtained. When crosslinking, the hydrogels can be formed by incorporating conductive polymers and metals, such as nanoparticles or CNTs, to form conductive networks with the polymer that show strong interaction between the conductive material and the polymer networks.

### 3.1. 3D Printing Method

The use of 3D printing technology allows for the convenience of building and designing sophisticated, tangible scaffolds. Crosslinking in 3D printing determines the precision of the advancement of hydrogel and the mechanical characteristics of the final product. Further, the roles of polymer ink treatment before the 3D printing process and the curing process after the printing process are important in improving mechanical properties.

**Table 3.** Cellulose-based 3D printed structure.

| Material | Printing type | Ionic conductivity | Young's moduli | Application | Ref. |
|---|---|---|---|---|---|
| CNCs, polyacrylic acid (PAA), choline chloride, ethylene glycol | Inkjet | 0.047 S $m^{-1}$ | 1.23 MPa | Auxetic strain sensor | [79] |
| Cellulose, NaOH/urea solvent | Inkjet | – | 11.1 ± 2.2 MPa | Thermal insulation material | [80] |
| CNFs, CNT | Inkjet | 216.7 ± 10 S $cm^{-1}$ | 247 ± 5 MPa | Wearable electronic devices | [81] |
| CNCs, choline chloride, acrylic acid (AA) | Extrusion | 0.011 mS $cm^{-1}$ | – | Tactile sensor | [82] |
| CNC, CNT | Extrusion | 0.01 S $cm^{-1}$ | – | E-skin sensor (150% strain) | [83] |
| CNFs, poly(acrylamide-*co*-acrylic acid)$_D$ | DLP | 0.83 S $m^{-1}$ | 4.12 MPa | Strain sensor | [84] |
| CNCs, CDs | DLP | – | 13.6 ± 4.2 kPa | Real-time monitoring of cell migration and differentiation | [85] |

Hydrogel 3D printing technologies are broadly categorized into inkjet printing, where print material is dispensed through nozzles to form individual layers and precise control of local pressure or force is used to print onto the lower layers; extrusion printing, which involves continuous driving of elastic print material through nozzles in filament form to print layer by layer; and digital light processing (DLP) printing, a noncontact method using a predesigned pattern exposed by a laser beam (UV, IR, or visible light) to fabricate liquid polymers through crosslinking. To use as polymer ink for 3D printing, the properties of the printing biomaterials must be tuned to match the processing methods, shrinkage, and stability of the obtained design, unlike the method of directly producing hydrogels in a solvent.[77] The simplest method is freeze drying, but it is expensive and might be transformed due to its ice crystal formation during the freeze-drying step to create pore structures to maintain geometric shapes. Depending on the reinforcing material employed, which in this case is anisotropic, such as the CNCs, viscosity and printability are reinforced, leading to the capability to maintain the shape of the scaffold that you want when dried at room temperature (**Figure 2a**). As to 3D printing with BNCs, the air-liquid interface should be controlled to be provided oxygen to meet the requirement. One study used a hydrophobic and immiscible solid matrix and CNFs hydrogel ink containing bacteria to help in the creation of an air–hydrogel interface and avail oxygen to the ink-containing bacteria amidst the matrix particle's gaps. As a result, oxygen levels were higher on the 3D-printed hydrogel surface facing the solid matrix and lower toward the center of the printed structure. Depending on the oxygen level difference, BNCs were biosynthesized, creating a porous composite region hydrogel with BNCs formed on the CNFs hydrogel surface (Figure 2b). In the case of 3D printing using materials with superelasticity and compressive resilience, it can be applied in fields such as energy storage, soft electronics, and sensors due to its potential for energy absorption.[78] One study produced a 3D-printed CNFs monolith that activated elastic behavior by competing with the strong hydrogen bonding network of CNFs when saturated with water, inducing a fully elastic structure. Additionally, incorporating hygroscopic salts into this monolith allowed control over moisture content, adjusting elastic behavior (Figure 2c). Applying the biocompatibility of cellulose to the complex shape formation of 3D printing enables its use as an intelligent platform, such as for cell migration monitoring. Another study created a noninvasive polymer hydrogel based on CNCs and carbon dots (CDs) using DLP printing, confirming that human skin cells could be tracked within the hydrogel for up to 30 d due to the unique fluorescence properties of CDs (Figure 2d).

In summary, cellulose, a biopolymer, is an excellent rheological modifier and can produce special surface shapes or overall (or detailed) shapes by adjusting the viscosity of solvents so that hydrogels can be designed and simulated through custom bioprinting according to various tissues and organs. Furthermore, increasing crosslink density and decreasing pore size of hydrogels based on cellulose content are significant advantages of polymer ink. However, caution is required due to the potential decrease in mechanical properties caused by defects resulting from pore formation, solubility with other substances, and uniformity of distribution when using cellulose. **Table 3** summarizes research on cellulose-based 3D printing.

### *3.1.1. Extrusion-Based 3D Printing*

Extrusion-based printing is a representative additive manufacturing (AM) 3D production technology known for its economy, versatility, and ability to create complex structures. It consists of fluid distribution and a computer-controlled automated robotic system, enabling precise material deposition based on 3D computer-aided design files.[86] In extrusion-based printing, the key points are the mechanical properties and shape fidelity determined by the adhesion between the printed layers. Variables such as layer height, line width, air gap, printing speed, and printing temperature exist in extrusion-based printing. Qualitatively, lowering the layer height increases back pressure, and increasing the printing speed decreases back pressure, which can improve roughness and accuracy.[87]

Additionally, since the purpose of scaffolds made with polymer ink is tissue regeneration, proliferation, and cell attachment, a microporous structure and interconnected pores are required.[88] Polymer inks are semi-solid, so viscosity plays a significant role in maintaining the shape of the structure during the drying process after printing.[89] High viscosity prevents droplet formation due to surface tension and prevents the collapse of the deposited structure. However, if the viscosity is too high, extrusion shear stress must be increased, which can affect the polymer inks' biological performance or drug retention capability. Thus, controls

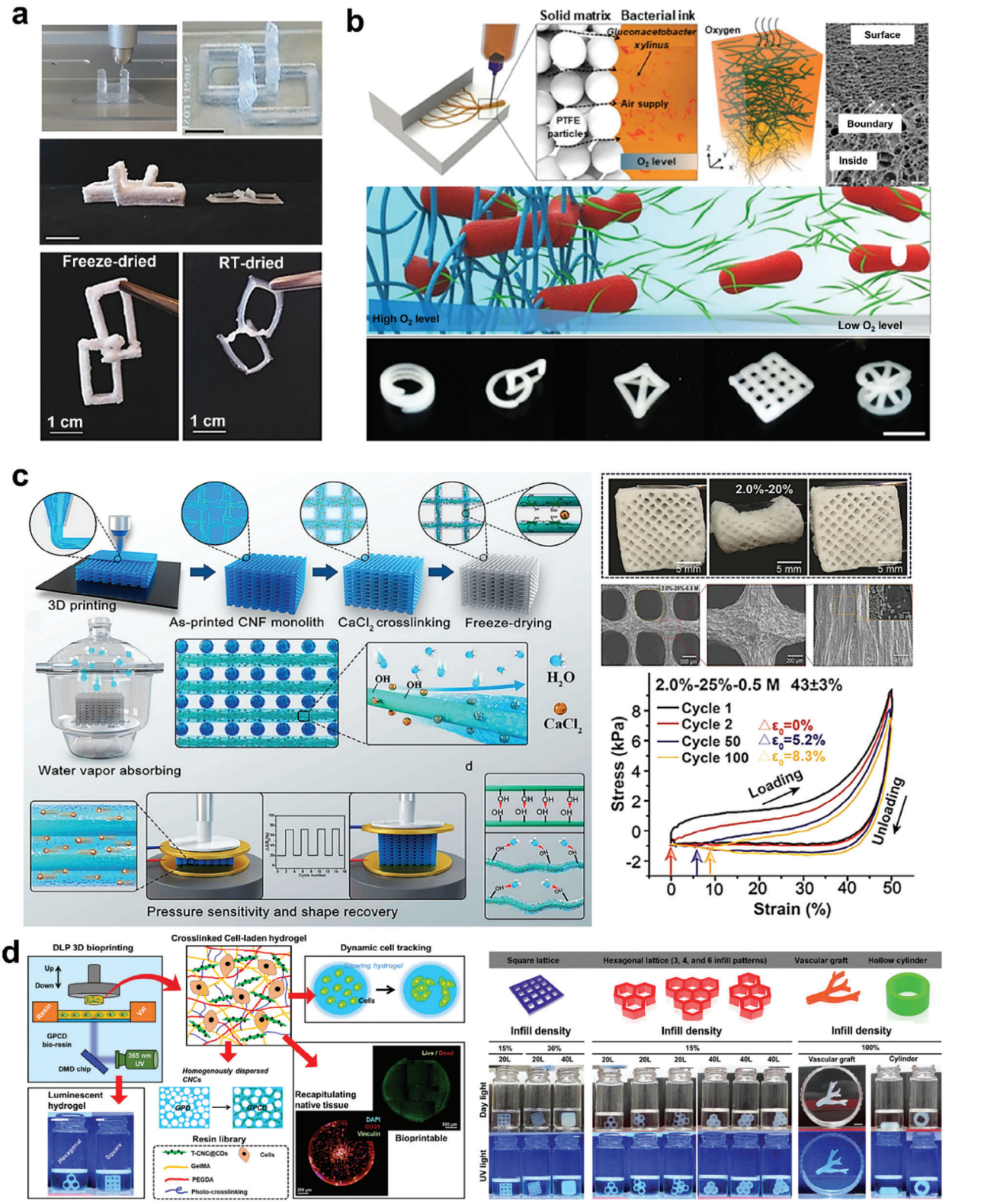


**Figure 2.** a) Freeze-drying method and room temperature (RT)-dried method with 0.2% surfactant added.[106] b) Solid matrix-based 3D printing with ink containing bacteria.[107] Copyright 2019, Nature Communications. c) 3D Printing of CNF Monolith, Followed by $CaCl_2$-Induced Crosslinking and Densification.[108] d) 3D printing of polyethylene glycol diacrylate (GPCD) bioresin.[85] Copyright 2023, Elsevier Ltd.

in the variables like the concentration of the polymer, molecular weight, and solubility need to be implemented so that the polymer ink has a fit viscosity.[90]

Furthermore, other factors that influence shape memory ability and cell growth when making a 3D scaffold include shear-thinning, yield stress, and the capability of the flow to structurally recover instantly whenever flow is ceased.[91] One study showed that the alignment of anisotropic CNCs is influenced by shear stress during printing, and shear-induced alignment along the printing direction was improved. A 20 wt% CNC hydrogel showed optimal rheological properties and was successfully printed into a 3D structure with high fidelity.[92]

The methods of using nanocellulose in extrusion-based printing can be divided into low concentration and high concentration. In scaffolds using low-concentration nanocellulose paste, preventing collapse and maintaining shape fidelity during printing and drying are important. One study used TEMPO-oxidized CNFs and gelatin methacrylate (GelMA) to create a low-concentration ink, producing a scaffold with excellent stability, cell compatibility, and adjustable mechanical strength through ionic interactions and UV crosslinking.[93] For high-concentration nanocellulose paste, research is ongoing to address mechanical properties and shape retention due to adhesion issues between printed layers caused by the high content of spherical particles.[94] One paper used high-concentration nanocellulose for 3D printing, and by controlling the drying conditions (relative humidity: 60% and 45%, temperature: 25 °C), created structures with excellent shape retention and improved mechanical properties.[95]

#### 3.1.2. Digital Light Processing-Based 3D Printing

Digital Light Processing (DLP) technology harmonizes digital video or image signals, light sources, and projection lenses to project the entire digital image onto a screen or other surface, adding layers through AM. This method projects cross-sectional images of objects layer by layer across the entire platform simultaneously, regardless of layer complexity, curing all points at once. This method offers high precision and high manufacturing speed, resulting in high cell viability.[96] In DLP, photopolymerization hydrogels occur under aqueous conditions, so a water-soluble photoinitiator plays an important role in determining 3D printing efficiency and the properties of the printed hydrogel object.[97] Therefore, using the DLP method requires combining a photosensitive resin with a photoinitiator or chemically modifying it into a resin form.[98] Insoluble and infusible thermosetting resins present issues of resource waste and environmental pollution due to single use, prompting recent research into reprocessable and reusable 3D printing resins.[99] Since cellulose itself does not have photopolymerization properties, it must be dispersed using solvents like dimethylformamide[100] or endowed with photopolymerization characteristics by binding acrylate or methyl methacrylate groups to the cellulose.[101] By substituting the hydroxyl groups (—OH) in cellulose with carboxymethyl groups (—$CH_2$—COOH) and methacrylation, the resulting methacrylated carboxymethyl cellulose (mCMC) enables cellulose to be used as a component of photocrosslinked hydrogels, making it applicable for DLP printing.[102]

#### 3.1.3. Stereolithography-Based 3D Printing

Stereolithography (SLA) is a 3D printing technique that uses the photocuring of liquid resins, similar to the DLP process. Unlike DLP, which employs a chip to project images to be used in the photopolymerization of the material, in SLA, a high-density UV laser is used to scan and photopolymerize the material. SLA uses laser light with a wavelength of 355 nm and is capable of proceeding with either radical or cationic photopolymerization.[103] The laser beam is positioned above the resin tank, and as the laser beam scans from above, the liquid resin solidifies. The platform lowers into the resin, with its surface corresponding to the layer thickness below the resin surface. The laser beam selectively traces along boundaries on the model and draws proper cross-sections to cure the resin. The platform then lowers layer by layer to repeat the process, resulting in the printing of a 3D scaffold.[104] In SLA, it is possible to incorporate nanocellulose as a filler for the SLA resin material to improve its mechanical and thermal performance.[105]

### 3.2. Gelation Methods

#### 3.2.1. Physical Crosslinking

Physical crosslinking is a method of producing hydrogels through ion/electrostatic interactions, noncovalent bonding, crystallization, hydrophobic interactions, etc., without the use of separate crosslinking agents.[109] Ion interaction is a crosslinking method that links polymer networks through the electrostatic force between hydroxyl groups of cellulose and cations.[110] It features adjustable crosslinking time and mechanical strength of hydrogels through concentration control. For divalent metal ions, the physical and chemical properties can be imparted depending on the metal ions used.[111] Electrostatic interaction is a crosslinking method that utilizes giant molecules with opposite charges to create polymer electrolyte complexes. Similar to the ion interaction method, the properties of hydrogels can be adjusted through the variable of polymer electrolyte[112] (**Figure 3a**). Forming hydrogels by utilizing the characteristics of specific substances can create reversible systems that can respond to environmental changes, extending the properties of hydrogels.[113] Polyvinyl alcohol (PVA) is crosslinked by using the crystallization (freeze–thaw cycle), where it is frozen and later thawed in the solvent; this form crossbinds through polymer chain crystallization that provides a highly covalent network as well as excellent mechanical properties[114] (Figure 3b). Hydrogen bonding, which plays a central role in important biological processes such as DNA replication, molecular recognition, and protein folding, is an excellent crosslinking method for producing supermolecular hydrogels with outstanding mechanical properties and directionality.[115] Since cellulose surfaces have numerous hydroxyl groups, cellulose-based hydrogels formed via hydrogen bonding exhibit excellent mechanical properties, self-healing properties, and pH responsiveness[116] (Figure 3c). In the case of hydrophobic interactions, hydrogels that are created when hydrophobic chains, usually folded, are exposed to aqueous solutions possess very stable properties, with good mechanical qualities provided through microphase separation

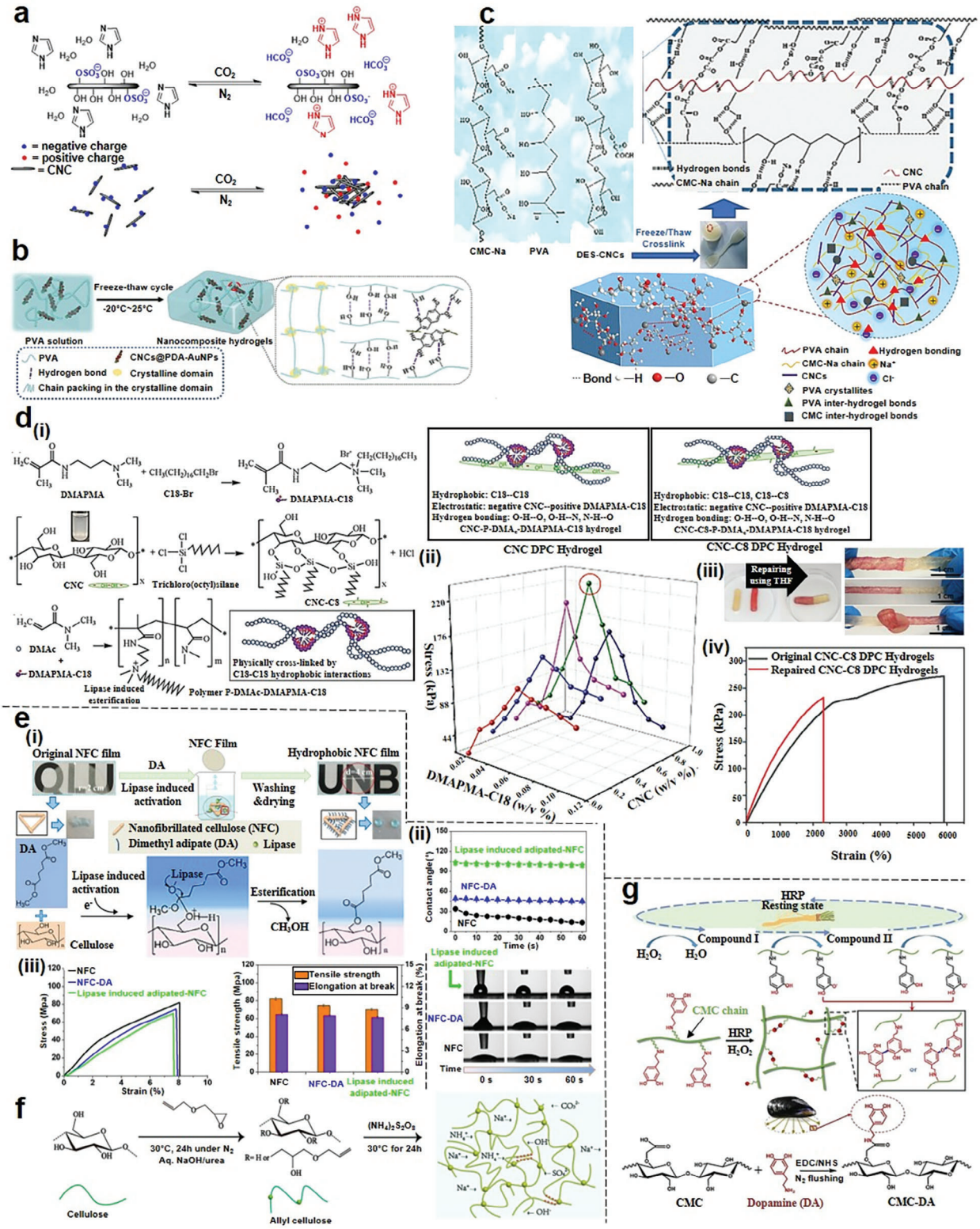


**Figure 3.** a) Schematic diagram of a nanocellulose-based hydrogel physically crosslinked with electrostatic interaction.[137] Copyright 2018, American Chemical Society. b) Schematic diagram of a nanocellulose-based hydrogel physically crosslinked with crystallization.[138] Copyright 2023, Elsevier Ltd. c) Schematic diagram of a nanocellulose-based hydrogel physically crosslinked with hydrogen bonding.[139] Copyright 2022, Elsevier Ltd. d,i) Schematic diagram of a nanocellulose-based hydrogel physically crosslinked with hydrophobic interaction.[140] Copyright 2021, Wiley-VCH. ii) Graph of mechanical properties of dual physically cross-linked (DPC) hydrogel according to dosage of CNC (or CNC-C8) and *N*-[3-(dimethylamino)propyl]methacrylamide

networks[117] (Figure 3dii–iv). Nanocellulose has the capability of making hydrogels through hydrophobicity through the formation of hydrophobic groups through chemical modification of the constituent hydroxyl groups to using hydrophobic interactions (Figure 3di). Hydrogels formed through hydrophobic interaction present synergistic effects with other physical crosslinking methods, showing enhanced performance and offering significant advantages in multiple crosslinking possibilities.[118]

Physical crosslinking is simpler to manufacture and less costly compared to chemical crosslinking when excluding raw materials. Additionally, since no chemical crosslinking agents are used, it is easier to recycle. It can avoid potential risks associated with toxicity, thus offering expectations of stability for substances such as cells and proteins.[119] However, achieving high mechanical strength remains a significant challenge for physically crosslinked hydrogels. One of the ways to complement this is double network hydrogels, which exhibit excellent mechanical strength even when fully physically crosslinked, thanks to effective energy dissipation.[120] Furthermore, hydrogels mechanical properties may be improved with polymer electrolytes,[121] nanocomposite reinforcement,[122] or natural polymers like lignin.[123]

#### 3.2.2. Chemical Crosslinking

Chemical crosslinking involves the use of substances that form radicals either by crosslinking agents or stimuli to chemically form chains between molecules and polymers (covalent bonding) to manufacture hydrogels, which are permanent and possess high bonding strength. Due to the covalent bonds formed, these hydrogels exhibit excellent structural stability and mechanical properties. Chemical crosslinking is achieved through processes such as free radical polymerization, esterification, and enzyme-catalyzed reactions. Free radical polymerization activates monomers into free radicals through external factors (light,[124] radiation,[125] frequency,[126] or initiators[127]), leading to copolymer formation by polymerization with other monomers. Esterification involves the reaction of carboxylic acids or hydroxyl groups with alcohols to form esters, which serve as crosslinking. It can be seen as one of the reactions that chemically modify the surface of cellulose,[128] providing reversible characteristics to hydrogels[129] (Figure 3ei). In this process, the hydrophilic hydroxyl group of cellulose is partially replaced by the hydrophobic ester group and the aliphatic group (Figure 3eii), and the tensile strength tends to decrease slightly (Figure 3eiii). Radical polymerization provides ease of gelation, allowing the creation of giant molecules by converting biopolymers into reactive groups, thus imparting ease of use and cell compatibility[130] (Figure 3f). Enzymatic catalysis can manipulate the kinetics of gel formation based on the chemical, stereochemical selectivity, and location of the enzymes[131] (Figure 3g). Additionally, enzyme-catalyzed crosslinking exhibits excellent mechanical properties without increasing cytotoxicity.[132]

The crosslinking agents in chemical crosslinking offer the advantage of adjusting the characteristics of hydrogels by controlling the crosslinking conditions, resulting in the stability conferred by the permanent bonding of hydrogels. However, some chemical substances following crosslinking possess potential toxicity. Synthetic crosslinking agents (such as *N,N'*-methylenebisacrylamide and glutaraldehyde) pose risks of cytotoxicity and pollute the environment depending on their handling.[133] Natural compounds (dialdehyde starch,[134] tannic acid,[135] genipin,[136] etc.) can serve as solutions to this issue. Furthermore, natural compounds can impart hydrogel properties, such as antimicrobial and anti-inflammatory effects, promoting wound healing.

## 4. Nanocellulose-Based Conductive Hydrogel

Nanocellulose can form structures utilizing conductivity from the production process, enabling the development of more sophisticated biomimetic nanomaterial composites or the design of high-performance materials. In one study, the orientation of CNFs was controlled and fixed by employing electrophoretic and electrochemical deposition techniques where the voltage was increased or decreased to obtain the CNF orientation in horizontal, random, or vertical positions with the anode side surface. It was confirmed that a complex shape with a CNF hierarchical structure having different layer directions could be formed through a one-pot process (**Figure** 4ai,ii). This nanocellulose is an excellent material for use as a platform for biosensors due to its excellent biocompatibility and conductive properties. Furthermore, it can be used not only in flat electrodes but also in 3D electrodes, and CNF hydrogels such as 3D plant stem can be manufactured by combining thin wire electrodes and plate electrodes (Figure 4aiii). In one study, TEMPO-oxidized CNF was used to make an acrylate-based hydrogel to confirm conduction changes and physical changes of the hydrogel with temperature (25 and −25 °C) (Figure 4bi). This hydrogel quickly gelled by free radical polymerization starting with Fe 3+ at room temperature, showing a bright red color (Figure 4bii). Figure 4biii is a graph showing the comparison of performance (Electrochemical impedance spectroscopy (EIS), conductivity, etc.) of hydrogels with different glycerol contents.

Conductive properties can be improved to nanocellulose by incorporating conductive materials, including CNTs, graphene, or carbonization using methods such as conductive polymer coating, conductive metal coating, carbonized, and CNT composite.[45] Conductive polymers offer flexibility and excellent electrical and optoelectronic characteristics with the advantage of easy adjustment. Conductive metals provide excellent conductivity along with chemical and thermal stability. Carbonization

(DMAPMA)-C18. iii) Photo of CNCDPC hydrogel self-therapy and deformation by external force. iv) Stress–strain graph of hydrogel. e,i) Schematic diagram of a nanocellulose-based film chemically crosslinked with esterification.[141] Copyright 2022, Elsevier Ltd. ii) Contact angle graphs and photographs of NFC, NFC-DA, and lipase-induced adipate-NFC films. iii) Graph of mechanical properties of nanofibrillated cellulose (NFC), NFC-dimethyl adipate (DA), and lipase-indicated-NFC films. f) Schematic diagram of a nanocellulose-based hydrogel chemically crosslinked with free radical polymerization.[142] Copyright 2019, American Chemical Society. g) Schematic diagram of a nanocellulose-based hydrogel chemically crosslinked with enzyme-catalyzed reaction.[143] Copyright 2019, Elsevier Ltd.

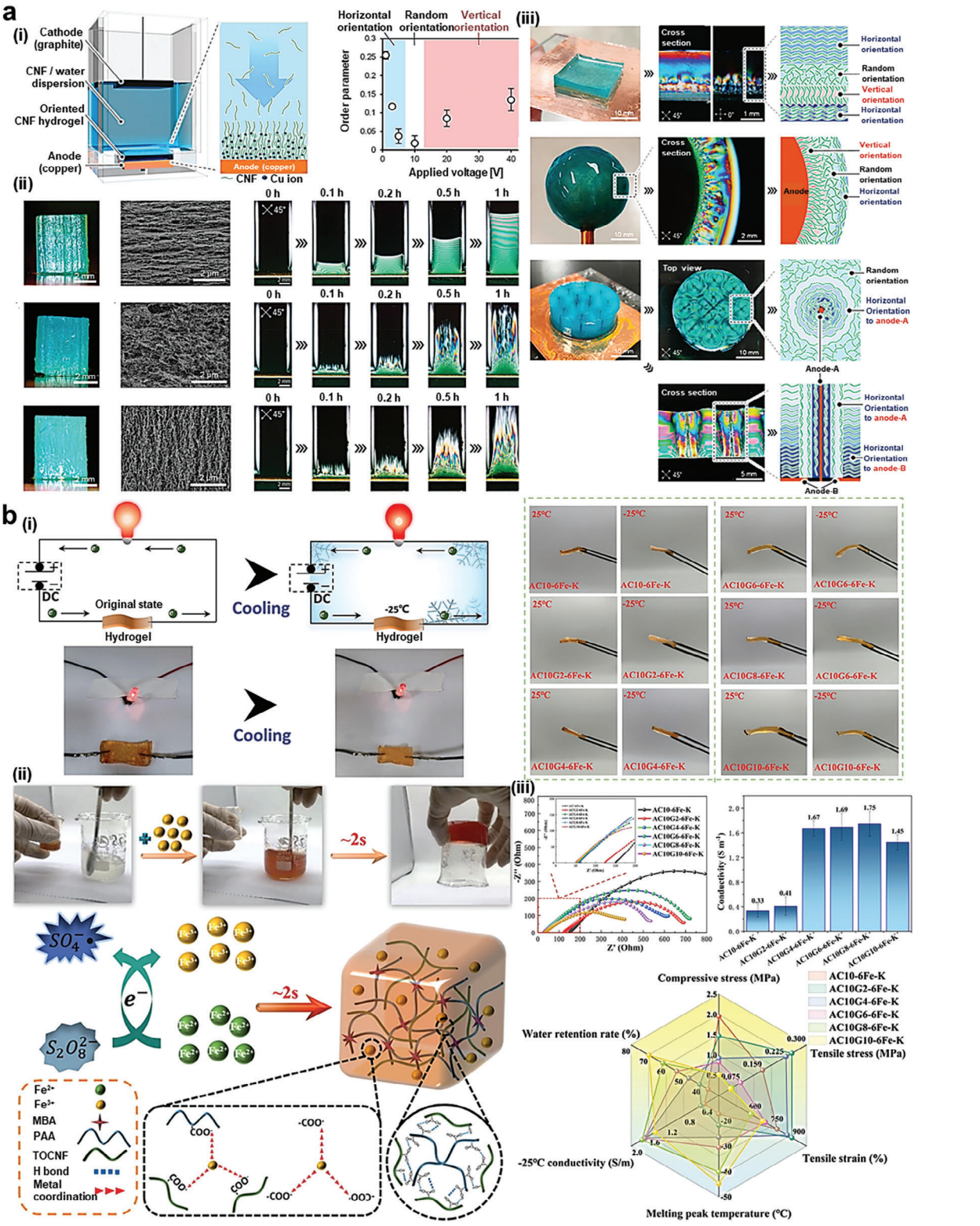


**Figure 4.** a) Oriented CNFs hydrogel.[146] Copyright 2022, American Chemical Society. i) Schematic diagram showing the formation at the anode by applying a DC voltage between the CNF/water dispersion. ii) Oriented CNFs hydrogels prepared at different voltages (1, 10, and 40 V). iii) Multilayer CNFs hydrogel and CNFs hydrogels were prepared using spherical and planar electrodes. b) Resistance change of acrylic-based TOCNFs hydrogel according to glycerol content or temperature.[147] Copyright 2024, Elsevier Ltd. i) Image of light emitting diode (LED) brightness and shape comparison according to temperature. ii) Schematic diagram of hydrogen bonding and metal ion coordination mechanisms during gelation. iii) Graph of performance comparison according to glycerol content.

enhances the porosity of nanocellulose, imparting more reactivity and providing energy storage and conversion properties. Through synthesis with nanocellulose, CNT dispersibility can be improved to create a self-supporting structure, resulting in a material with excellent electrical conductivity and mechanical strength. Blending and surface grafting with electroconductive materials are the primary methods of fabricating nanocellulose-based conductive structures.[144] The blending method involves mixing various materials where the physical interactions among the blend constituents allow stability and charge transfer.[145]

### 4.1. Imparting Conductivity with Conductive Polymers

Polyaniline (PANI) exhibits pseudocapacitance, which arises from the redox process where doped ions are reversibly adsorbed and desorbed from the polymer chains. However, electrodes based on PANI experience structural instability (both chemically and mechanically) due to the repetitive volumetric expansion and contraction of PANI during charge/discharge cycles.[148] This disadvantage can be inhibited by incorporating nanocellulose[149] (**Figure 5**ai–iii).

Poly(3,4-ethylenedioxythiophene): poly(styrene sulfonate) (PEDOT: PSS) is acknowledged as an appropriate conductive polymer for commercialization based on material solubility, stability, and processability as well as the high electrical conductivity.[150] The morphology of PEDOT: PSS dispersion typically consists of a PEDOT-enriched core and a PSS polyanion shell arranged in a coiled-like and randomly oriented structure.[151] In one study, a mixture of BNCs and this material was used for cell regeneration experiments. Cell toxicity tests showed no observed cell death and it was found to be more successful than other substances, such as indium tin oxide (ITO) or gold (Au).[152] Furthermore, this composite material was reported to be effective in drug delivery. The research results indicate that the composite material appropriately retains drug molecules, exhibiting a linear release curve, thus enabling controlled release.[153] In other study, cellulose-based substrates exhibiting high mechanical properties, electrochemical capacity, and cell attachment were fabricated utilizing excellent doping between PEDOT and $Cu^{2+}$ (or $Zn^{2+}$) (Figure 5bi–iv).

Polyacrylamide (PAAM) typically exhibits strong hydrophilicity due to the presence of amide groups.[154] Because of its nontoxicity, mechanical strength, ease of adjusting biophysical and chemical properties, and facile chemical modification, it has been widely utilized in the preparation of various functional hydrogels (Figure 5ci–iv). These properties can facilitate effective dispersion by weakening the aggregation of functional materials, such as CNTs, during hydrogel fabrication, thereby allowing hydrogel to be used as an advanced actuator.[155] In one study, a hydrogel was produced by mixing CNCs and CNFs with PAAM, and biocompatibility and cytotoxicity tests were conducted. This test showed that hydrogels incorporating both CNCs and CNFs with PAAM supported cell proliferation to a higher extent than PAAM hydrogels.[156] This study indicates that PAAM has been used in this study and is compatible with CNCs and CNFs. The obtained mixture is safe and effective with respect to wound healing application. In another study, lithium chloride (LiCl) was added together with another study and PAAM to create a hydrogel with ion transport conductor properties. The hydrogel showed high transmittance (≈91.2%) and high biocompatibility and the hybrids' multifunctional sensors enable wide-range strain sensing capability (gauge factor, ≈3.8) over a wide temperature range (from −20 to 60 °C), underwater information transmission, and real-time temperature (temperature coefficient of resistance, roughly $-1.1\%\ °C^{-1}$) responsiveness.[157]

PVA, obtained through the hydrolysis of vinyl acetate, is a biocompatible, biodegradable, and nontoxic polymer widely used in medical applications due to its elasticity and chemical stability at room temperature (Figure 5di–iii). In one study, researchers mixed nanocellulose and PVA to produce hydrogels for wound dressings. These hydrogels exhibited high moisture retention and absorption properties, suggesting good prospects for use in wound dressing. Additionally, the study demonstrated the high biodegradability of the hydrogels in soil, making them sustainable and environmentally friendly materials. Furthermore, using rats, the efficacy of wound healing was evaluated, demonstrating the excellent wound-healing properties of PVA and nanocellulose.[158]

### 4.2. Imparting Conductivity with Carbon-Based Materials

CNTs have been widely utilized as the basic building blocks for constructing flexible and conductive materials, owing to their remarkable mechanical properties and electrical conductivity, since their discovery. However, they often face challenges such as poor dispersion and severe aggregation due to their inherent hydrophobic nature. Nanocellulose exhibits a strong affinity for CNT, making it highly attractive for developing flexible hybrid materials. In these hybrids, nanocellulose aids in achieving uniform dispersion of CNT, and CNT can impart specific properties to nanocellulose, allowing for more tunable modulation of morphological structure and mechanical properties.[163] In one study, an excellent wound-healing dressing was used by BNCs and multiwalled carbon nanotubes (MWCNT). This freeze-dried hydrogel demonstrated rapid healing of diabetic wounds and exhibited excellent vascular regeneration and complete re-epithelialization of wounds.[164] In another study, CNCs were grafted with phenylboronic acid (CNCs-ABA) via a two-step method involving excessive periodate oxidation and reductive amination, enhancing stabilization onto MWCNT (**Figure 6**ai). Furthermore, leveraging the synergistic effect of MWCNT and NaOH, conductivity was increased to confirm rapid resistance change detection, therapeutic effects, and shape memory due to MWCNT's photothermal effect (Figure 6aii–vi).

The cellulose-based matrices, including hydrogels or scaffolds, have been incorporated with graphene oxide (GO) and its derivatives, wherein they can stabilize the structure of nanocomposites and improve the mechanical properties of the nanocomposite system.[165] Chemically crosslinked graphene oxide-nanocellulose (GO-NC) nanosheet domains with noncovalent interactions (hydrogen bonding, hydrophobic, and CH-$\pi$ stacking) exhibit enhanced elasticity, flexibility, and significant hydrogel deformation resistance. Alongside robust GO nanosheets, these hydrated species serve as physical crosslinking points, absorbing and dissipating energy during deformation, thus synergistically enhancing the strength and resilience

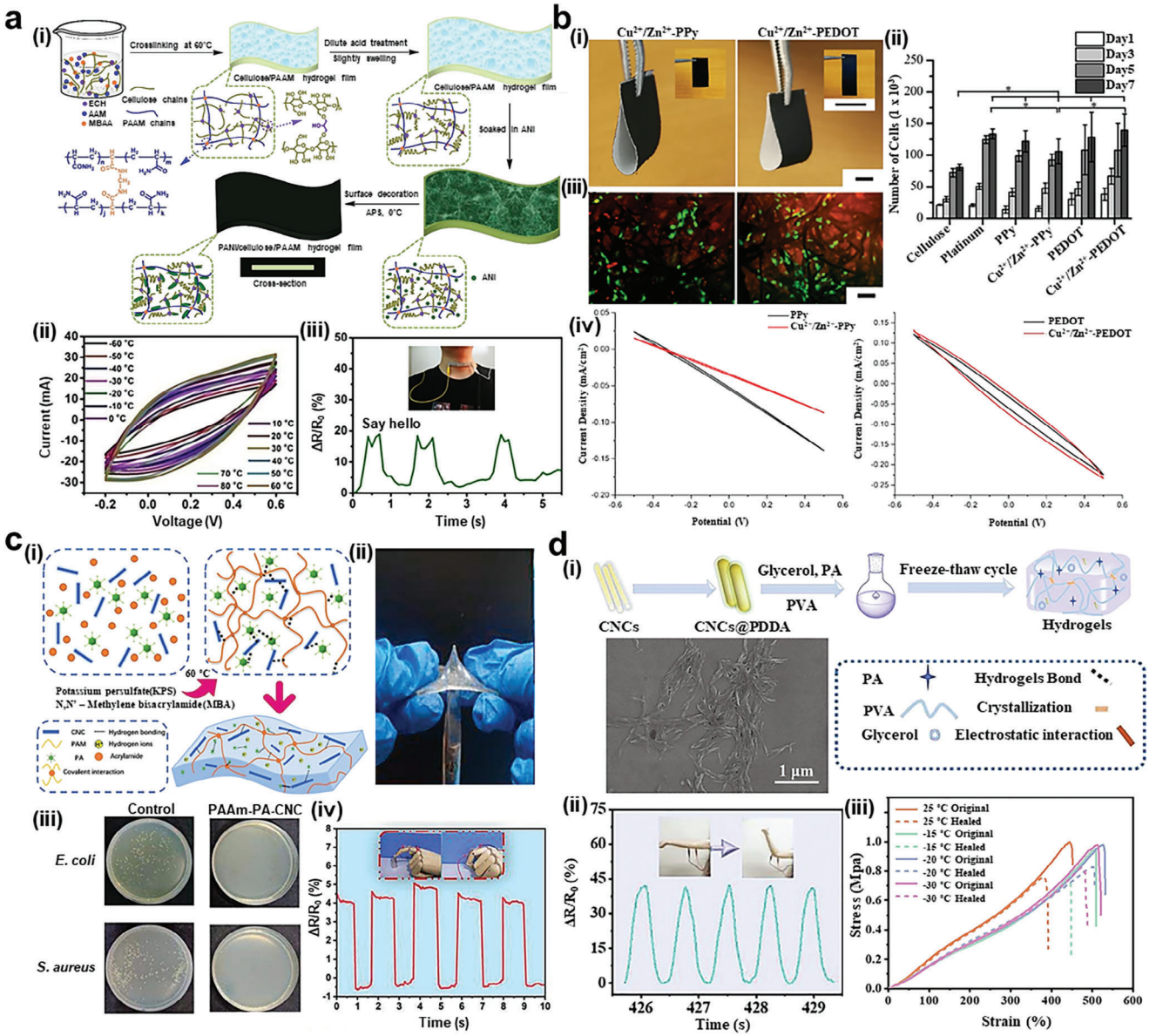


**Figure 5.** Nanocellulose-based conductivity hydrogel: Conductive polymers. a) PANI/cellulose/polyacrylamide hydrogels.[159] Copyright 2021, Elsevier Ltd. i) Schematics of the preparation route of the hydrogel. ii) Cyclic voltammetry (CV) curves of the hydrogel (supercapacitor) at various temperatures. iii) The response was speaking "Hello," respectively. b) electroactive($Cu^{2+}/Zn^{2+}$-PPy, $Cu^{2+}/Zn^{2+}$-PEDOT) cellulose-based substrates.[160] Copyright 2020, Elsevier Ltd. i) Images of electroactive cellulose-based substrates. ii) Cell proliferation over 7 d at pH 7.5 condition. iii) Representative images of HaCaT cells stained with fluorescein diacetate (FDA) and propidium iodide (PI) on day 7 at pH 7.5 condition. iv) Representative cyclic voltammetry graphs of the substrate post-cellular studies at pH 7.5 condition. c) PAAm-PA-$CNC_{0.1}$ hydrogels.[161] Copyright 2022, Elsevier Ltd. i) Structural schematic of PAAm-PA-$CNC_{0.1}$ hydrogels. ii) Photographs demonstrating the hardness of the hydrogel. iii) Antibacterial evaluation of the hydrogel in this work against *E. coli* and *S. aureus*. iv) The change in $\Delta R/R_0$ of the hydrogel sensor during wrist movement at −15 °C. d) PVA/CNCs@poly(diallyldimethylammonium chloride)/phytic acid hydrogels.[162] Copyright 2022, Elsevier Ltd. i) Schematic illustration of the fabrication of the hydrogel. ii) Hydrogel sensors for elbow bending detection. iii) The stress–strain curves of the hydrogels with assorted temperatures.

of the hydrogel. In one study, a double-crosslinked cellulose-GO (DCCG) nanosheet composite hydrogel with photothermal antibacterial performance was created through hydrogen bonding and hydrophobic interactions (Figure 6bi,ii). When exposed to near-infrared radiation, GO-NC hydrogels demonstrate broad-spectrum and potent antibacterial effects against Escherichia coli and Staphylococcus aureus (Figure 6biii–vii). Other studies, drawing inspiration from muscles, the combination of a rigid GO-NC network with a flexible poly [acrylamide-*co*-(acrylic acid)] (poly (AAm-*co*-AAc)) network in a dual-network hydrogel (GO-NC-poly (AAm-*co*-AAc)) yields outstanding flexibility and deformability (Figure 6ci,ii). With reversibly interconnected microdomains between conductive components, the GO-NC-poly (AAm-*co*-AAc) hydrogel exhibits remarkable durability and

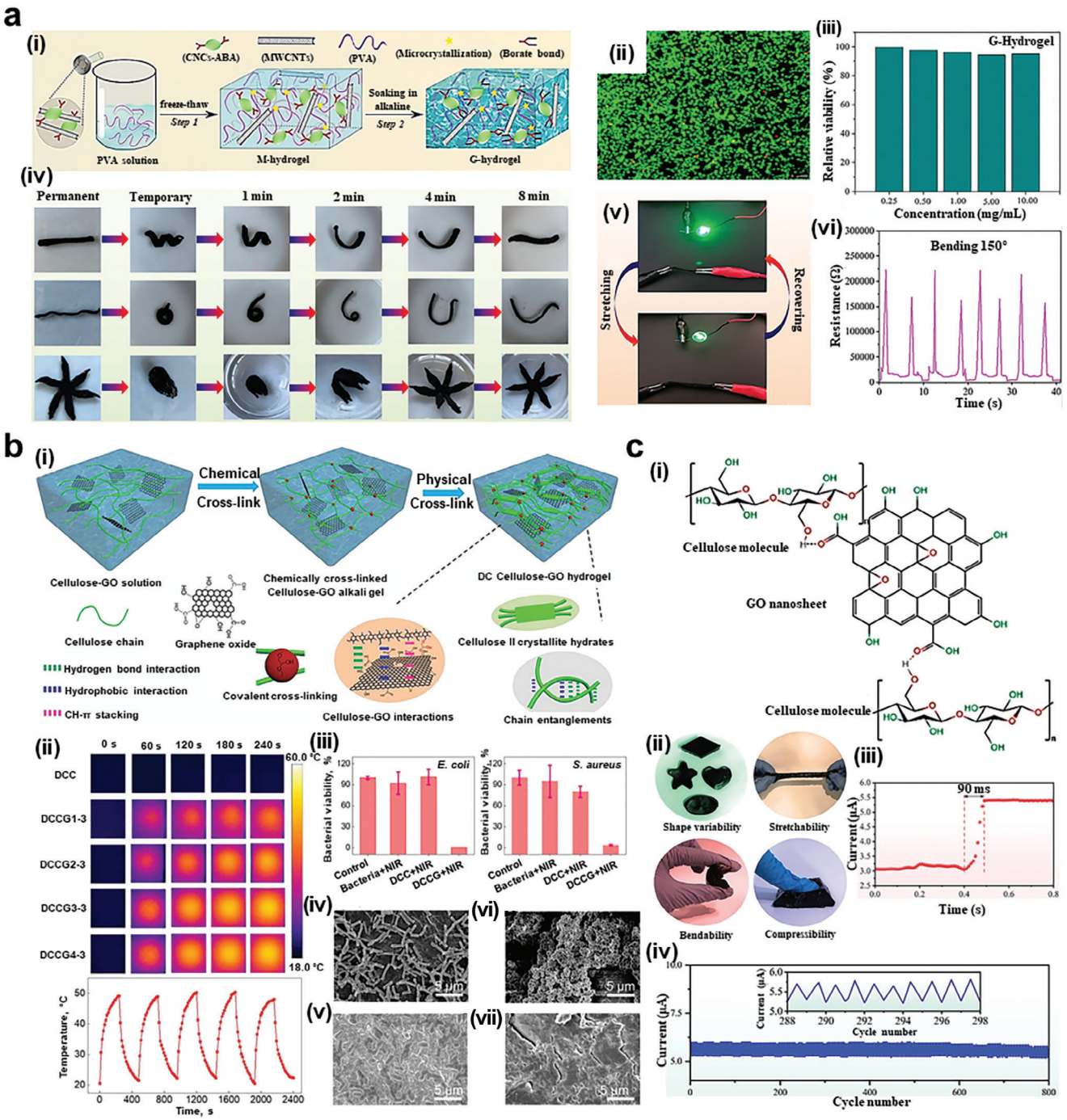


**Figure 6.** Nanocellulose-based conductivity hydrogel: Carbon-based materials. a) CNCs-ABA/MWCNT/PVA hydrogels.[166] Copyright 2022, Elsevier Ltd. i) Schematic illustration of the hydrogel. ii) Fluorescence pictures and iii) histograms of live/dead L929 cells cultured at the hydrogel. iv) Photographs of shape memory behavior of the hydrogel. v) Brightness changes according to stretch of the hydrogel. vi) Resistances change according to the bending of the hydrogel. b) double-crosslinked cellulose–GO(DCCG) nanosheet composite hydrogels.[167] Copyright 2022, Elsevier Ltd. i) Schematic illustration of the hydrogel. ii) Thermal infrared images of the hydrogel with different GO contents at a power density of 2 W $cm^{-2}$ under 808 nm laser irradiation and photostability of DCCG2-3 during alternating on–off light irradiation (2 W $cm^{-2}$) for five cycles. iii) Bar graphs showing the relative bacterial survival of *E. coli* and *S. aureus*. scanning electron microscope (SEM) images of iv, v) *E. coli* and vi, vii) *S. aureus* on DCCG4-3 iv, vi) before and v, vii) after near-infrared (NIR) irradiation. c) GO@NC-poly(AAm-*co*-AAc) hydrogels.[31] Copyright 2022, Elsevier Ltd. i) Schematic illustration of possible hydrogen bonds between GO sheets and cellulose molecules. ii) Optical images to show the shape variability, stretchability, bendability, and compressibility of the hydrogel. Self-healing property of the muscle-inspired hydrogel and their application for sensors. iii) Response time. iv) Durability test for 800 cycles.

repeatability during stretching-releasing processes, benefiting dynamic stability in strain sensors and suitability as a monitoring sensor for sensitive response detection to movement (Figure 6ciii,iv).

### 4.3. Imparting Conductivity with Carbon Dots

Carbon dots (CDs), as a kind of carbon-based luminescent material, are gradually becoming the new generation of luminescent substances due to their abundant resources, low toxicity, and environmentally friendly properties and they have extensive development prospects in the substitution of commercial organic fluorophores. They are being recognized as successors to quantum dots. Particularly promising for photothermal therapy (PTT), CDs have been evaluated for their reported thermal conversion efficiency exceeding 50%. However, they have not been considered efficient materials for photodynamic therapy (PDT). Consequently, efforts have been made to enhance PTT/PDT effects by incorporating small molecule photosensitizers onto CDs or grafting them onto CDs surfaces. **Figure** 7ai shows the schematic illustration of the preparation of the hydrogel. The hydrogel exhibited promising photothermal and cell compatibility characteristics when examined in vitro and in vivo studies (Figure 7aii–iv). In one study, a hydrogel was fabricated by mixing CDs with CNCs. This hydrogel, reported to be more convenient to manufacture compared to other injectable hydrogels, offers a simpler production process for phototherapy agents. Importantly, the synthesized hydrogel achieved significantly higher efficiency in both PTT and PDT simultaneously, eliminating the need for complex modifications of phototherapy agents. Thus, the direct interaction between the phototherapy agent and the matrix not only provides a new strategy for the production of injectable hydrogels but also opens up new avenues for advanced tumor treatment.[168] In another study, a fluorescent hydrogel was developed using CDs and CNFs.

Interestingly, this hydrogel exhibited different colors depending on the wavelength of light, including visible light and ultraviolet light. Furthermore, this hydrogel, when placed in a glucose solution and subjected to an electric current, was able to sense glucose, making it suitable for various sensing purposes. Thus, the nanocomposite of nanocellulose and CDs allows the development of hydrogels with multiple sensing applications (Figure 7bi-ii).

### 4.4. Imparting Conductivity with Transition-Metal Carbides/Nitrides

The 2D family of layered transition metal carbides, nitrides, or carbonitrides known as transition-metal carbides/nitrides (MXenes) is exfoliated from their parent MAX phases using selective wet chemical etching procedures. MXenes with special mixing functions of metal (transition metal atom) and ceramic (carbon/nitrogen atom) have superior surface chemistry, so they show exceptional mechanical stability, good thermal conductivity, and high metallic conductivity up to 6000–8000 S $cm^{-1}$.[170] In addition, features such as good hydrophilicity and adjustable surface functional groups serve as suitable hydrogel materials.[171] CNCs can protect MXenes, which are vulnerable to oxidation, so stable and water-dispersible hydrogel production is possible (**Figure** 8ai–iii). MXenes can provide excellent biocompatibility and antibacterial effects when constructing conductivity hydrogels like carbon-based materials. In one study, a hydrogel was manufactured by adding biosynthetic selenium nanoparticles (BioSeNPs) to CNC-MXenes (Figure 8bi). Its antibacterial properties were confirmed through the inversion zone method (Figure 8bii) and could be used as a sensitive strain sensor (Gauge factor (GF) = 6.24) (Figure 8biii). In another study, a hydrogel sensor was manufactured by adding tamarind gum (TG) and PAAM to CNC-MXenes (Figure 8ci). When the temperature increased to 43, 52, and 62 °C, the $\Delta R/R_0$ gradually decreased to 4%, 8%, and 12%, respectively. When the sensor was exposed to humidity, the $\Delta R/R_0$ initially increased gradually and then remained almost constant after the humidity flow stopped, indicating the sensor's ability to detect humidity (Figure 8cii). Additionally, it was confirmed that this hydrogel can stretch up to 2000% without damage and fully recover to its original state after external pressure (Figure 8ciii).

## 5. Application of Nanocellulose-Based Hydrogel

### 5.1. Wound Healing Dressing

The healing process of tissues involves a series of multiple interacting and complex phases that are aimed at rebuilding injured tissues. These stages can be divided into four interrelated phases: hemostasis, inflammation, proliferation, and remodeling. These phases occur temporally in a biological process with feedback mechanisms with a complex and interdependent sequence.[175] Our body possesses electrical conductivity, and when the skin is injured, the signal transmission between epithelial cells is disrupted.[176] In this scenario, the wound edge becomes the anode, and the central region becomes the cathode, generating an endogenous electric field that stimulates the movement and proliferation of fibroblasts.[177] Electrically conductive hydrogels promote this mechanism, enhancing antimicrobial activity and allowing controlled drug delivery.[178] They help restore skin conductivity and also help the skin fibroblasts move toward the site of the injury.[179] Electrically conductive hydrogels can also act as wearable sensors capable of detecting motion and other minute alterations in physiological signals[180] for the continuous monitoring of wound healing.[181]

Extracellular matrix (ECM) acts as a 3D network structure that provides cell adhesion, tissue, and cell protection from external forces and serves as a medium for the transmission of bioelectrical signals between cells or between cells and the substrate.[182] Signal transmission in this context involves innate voltage gradients for wound healing post-injury, ion flux, and the role of electric fields.[183] Using these aspects, the use of biocompatible conductive materials makes it possible to apply the principles of electrical stimulation to promote regulation, including the proliferation and differentiation of cells.[184] Due to the 3D network structure, biocompatibility, porosity, and a high level of moisture content in hydrogels, hydrogels enable the functioning of ECM. ECM hydrogels, through interactions between cells and ECM hydrogels such as cell infiltration and angiogenesis and regulation of macrophage behavior, promote the remodeling phase of wound

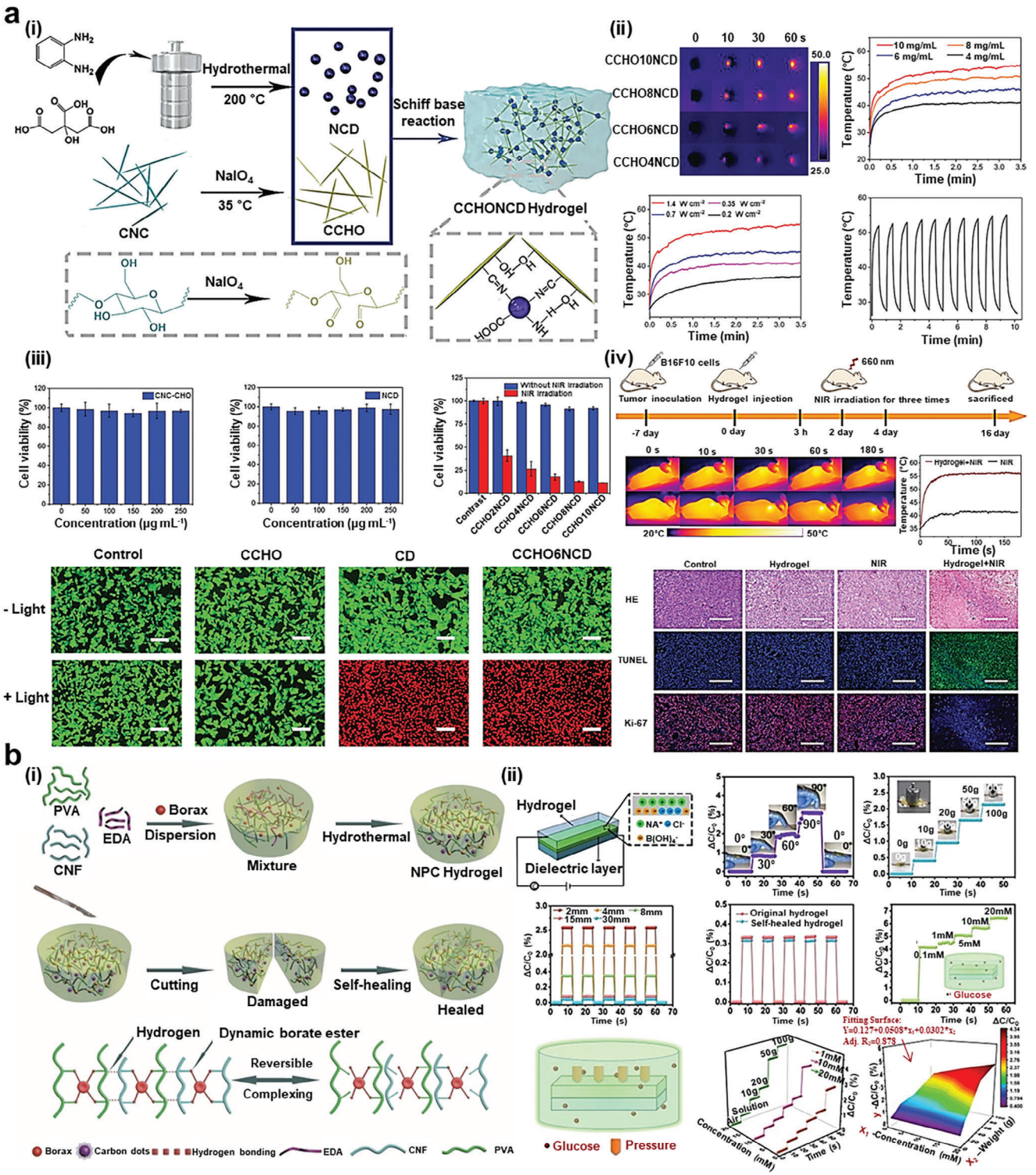


**Figure 7.** Nanocellulose-based conductivity hydrogel: Carbon dots. a) aldehyde-modified cellulose nanocrystal (CCHO)amido modified carbon dots (NCDs) hydrogels.[169] Copyright 2021, Wiley-VCH. i) Schematic illustration of the hydrogel. ii) Infrared thermal images of the hydrogels at different time intervals. iii, iv) In vitro and in vivo analysis of the hydrogel. Relatively, the cell viability of B16F10 was incubated with the hydrogels with or without 660 nm LED irradiation through CCK8 assays. Live/dead staining assay of B16F10 alone and treated with the hydrogel. b) nanocellulose/polyvinyl alcohol/carbon dot hydrogels.[33] Copyright 2021, Elsevier Ltd. i) Schematic illustration of the hydrogel. ii) Graphs of the properties and sensing efficacy of hydrogels.

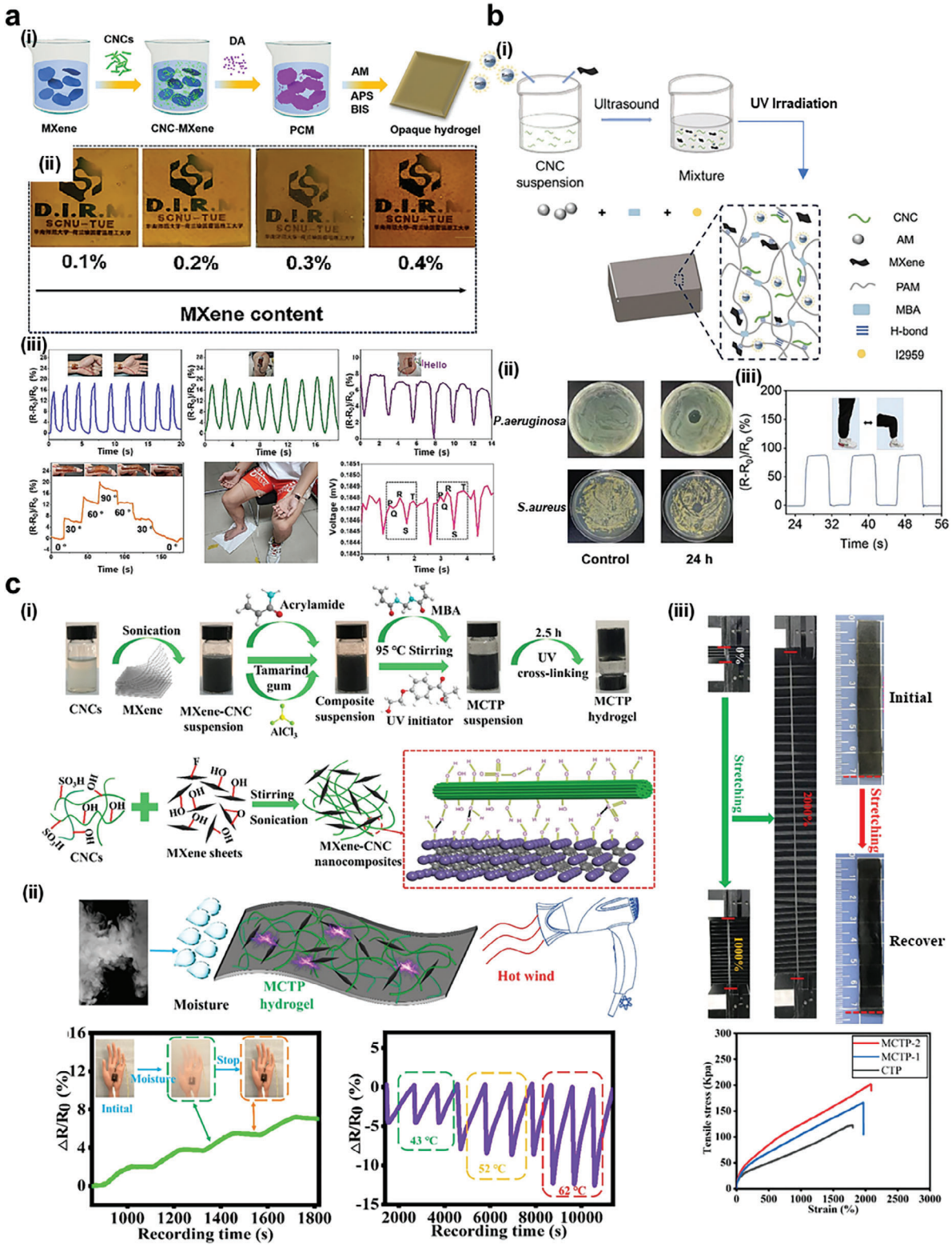


**Figure 8.** Nanocellulose-based conductivity hydrogel: MXenes. a) CNC-MXenes-PAAM hydrogel.[172] Copyright 2023, Elsevier Ltd. i) Schematic illustration of the hydrogel. ii) Photograph of transmittance according to MXenes content. iii) Graph of resistance changes with movement across different parts of the body. b) BioSeNPs-CNC-MXenes hydrogel.[173] Copyright 2024, Elsevier Ltd. i) Schematic illustration of the hydrogel. ii) Antibacterial properties of BioSeNPs-CNC-MXenes hydrogel. iii) Graph of resistance change with bending. c) CNC-MXenes-TG-PAAM hydrogel.[174] Copyright 2021, Elsevier Ltd. i) Schematic illustration of the hydrogel. ii) Graph of resistance changes with temperature and humidity in the hydrogel. iii) Photographs of the mechanical properties of hydrogel.

**Table 4.** Cellulose-based ECM mimetic scaffold.

| Cellulose type | Composite material | Conductivity | Application | Ref. |
|---|---|---|---|---|
| CNCs | Polypyrrole (PPy), AA, sodium *p*-toluene sulfonate (TsONa) | $8.8\times10^{-3}$ S cm$^{-1}$ | Catalyst support, neural regeneration, and carbon capture fields. | [186] |
| | Acellular gelatin, chitosan | – | Deposition and growth of human epidermal keratinocytes (HEKs) and human dermal fibroblasts (HDFs) | [187] |
| | Pectin, chitosan | – | Regeneration of cartilage tissue | [188] |
| | Silk fibroin, carboxymethyl chitosan, strontium substituted hydroxyapatite (SrHAp) | – | Increased expression of osteogenic gene markers | [189] |
| CNFs | PVA, PANI | $5.19 \pm 0.07$ S m$^{-1}$ | Adhesion and growth of mouse fibroblasts (L929) | [190] |
| | CNT, alginate | 0.12 S cm$^{-1}$ | Human neuroblastoma cells (SH-SY5Y) grow and differentiate into neuronal cells | [191] |
| | Sulfonated carbon nanotubes (SCNTs) | $5.2\times10^{-6}$–$6.2\times10^{-2}$ S cm$^{-1}$ | Composition of myocardial tissue engineering scaffold | [9c] |
| BNCs | PPy, CNT | $1.67\times10^{-3}$ S cm$^{-1}$ | Proliferation of mouse fibroblasts (NIH3T3) | [192] |
| | AuNP, chitosan | $6\times10^{-2}$ S m$^{-1}$ | Adhesion and viability of cardiomyoblasts (H9C2) | [193] |
| | PPy, pyrrole, PVA | $10^{-8}$–$10^{-2}$ S cm$^{-1}$ | Attachment and differentiation of H9C2 | [194] |
| | AuNP, PEDOT: PSS | $16.65 \pm 1.27$ S cm$^{-1}$ | Adhesion, growth, and proliferation of animal osteoblasts (MC3T3-E1) | [195] |
| | PVA, hexagonal boron nitride | – | Attachment and proliferation of human osteoblast cells (american type culture collection (ATCC)), 3D-printed functional scaffolds | [196] |

healing.[185] Cellulose, a natural polymer, exhibits excellent biocompatibility and is an easily manufactured material for hydrogel synthesis with conductive substances. **Table 4** shows cellulose-based ECM mimetic scaffolds applicable to biological contexts.

### 5.2. Stimuli-Responsive Shape Memory Polymers

Shape memory polymer (SMP) is a smart material capable of intuitively responding to stimuli by detecting external signals, undergoing a transition from a stimulus-free state to a temporary shape, and back again when stimulated. Shape memory is imparted not by inherent properties of a specific polymer but through the formation of a 3D network structure with net points/junctions, which prevents chain slippage/flow/creep during deformation via specific processing steps (molecular architecture, reversible mobility changes, conformational entropy, and programming).[197] The technology of maintaining a temporary shape and restoring it permanently upon stimulation is appealing in fields such as actuators, artificial muscles, and medical implants.[198] For instance, by fabricating SMPs containing biocompatible and biodegradable biomaterials, it becomes feasible to easily adapt to various irregular crack surfaces (wounds) without additional external force, facilitating the production of attractive dressings that accelerate wound healing processes and prevent secondary complications.[199] Thus, the primary purpose of incorporating cellulose into SMPs is to address the weak mechanical strength typically observed when using materials with shape memory induced by stimulation alone while also leveraging the advantages of natural polymers, such as biocompatibility and biodegradability. In particular, synthesizing hydrogel nanocomposites based on CNCs can promote structural anisotropy through CNC alignment, thereby enabling the preparation of programmable stimulus-responsive systems.[200]

One of the representative examples of thermoresponsive SMPs is poly(*N*-isopropyl-acrylamide) (PNIPAM), which undergoes a phase transition at a temperature similar to that of the human body (30 °C).[201] The molecular chains of PNIPAM consist of hydrophilic amide groups (—CONH—) and hydrophobic isopropyl groups (—$CH(CH_3)_2$) exhibiting hydrophilicity through hydrogen bonding between amide groups and water molecules at low temperatures and hydrophobicity when these hydrogen bonds are disrupted at high temperatures.[202] However, PNIPAM suffers from low printability and mechanical properties. Cellulose serves as an excellent reinforcement method for improving the mechanical strength of PNIPAM-based hydrogels, offering a superb security measure in the biofield as a biopolymer. By incorporating cellulose, it becomes possible to effectively enhance the expansion and mechanical properties of hydrogels without compromising flexibility and biocompatibility, thus creating hydrogels with interfacial bonding strength (**Figure 9ai**). Figure 9aii,iii is a schematic diagram showing the internal change of the hydrogel according to temperature and a graph of the current change accordingly. Another example, poly(*ϵ*-caprolactone) (PCL), exhibits properties such as shape memory and conductivity depending on temperature, making it sustainable and enabling the production of environmentally friendly cellulose-based composites. Demonstrates that deposition of Ag onto CNCs-PCL composites improves mechanical properties. High shape fixity and rapid shape recovery ability demonstrate stable and superior conductivity at various bending angles with rapid response rates.[203]

There is considerable interest in pH-responsive SMPs due to their ability to detect significant pH changes in specific areas of

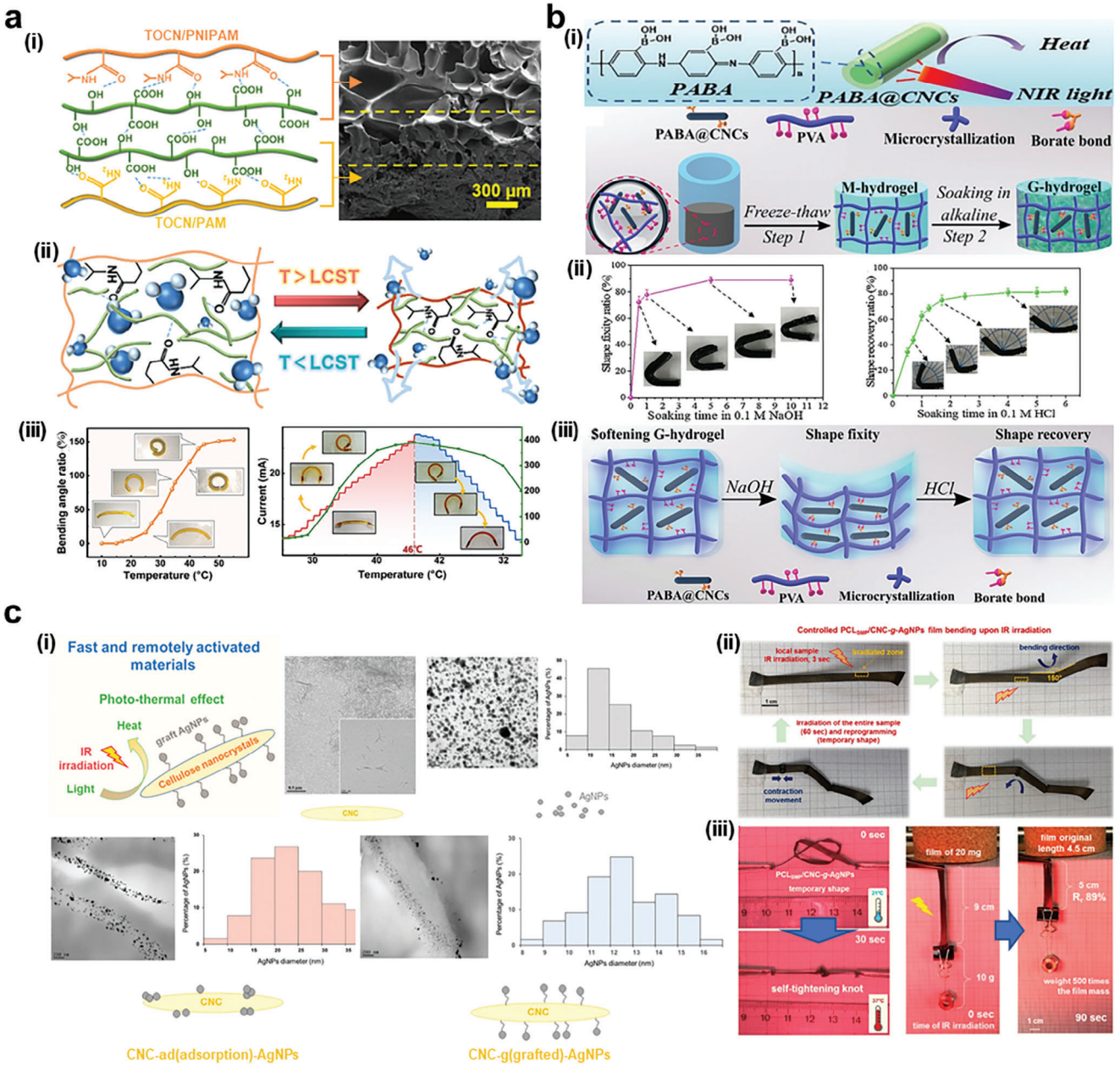


**Figure 9.** a) Nanocellulose-based thermo-responsive SMPs.[210] Copyright 2024, Elsevier Ltd. i) Structural schematic of PNIPAM/TOCN/PAM bilayer hydrogel. ii) Temperature response mechanism schematic of TOCN/PNIPAM hydrogels. iii) The bending angle ratio is a function of temperature (left) and curves of bending angle temperature and current temperature are detected in the actuator (right). b) Nanocellulose-based pH-responsive SMPs.[211] Copyright 2021, Elsevier Ltd. i) Structural schematic of polymerization of 3-aminophenylboronic acid (3-ABA) on CNCs. ii) Bending angle ratio as a function of soaking time in NaOH (left) HCl (right). iii) pH (NaOH, HCl) response mechanism schematic of poly(aminobenzeneboronic acid (PABA)@CNCs/PVA G-hydrogel. c) Nanocellulose-based IR-responsive SMPs.[212] Copyright 2018, American Chemical Society. i) Structural schematic of CNC-g(grafted)-AgNPs and transmission electron microscopy (TEM) micrographs of CNCs, AgNPs, CNC-ad-AgNPs, and CNC-g-AgNPs. ii) IR control of the bending direction upon local activation. iii) Self-tightening and contraction properties of the hydrogels upon IR illumination.

the body and facilitate drug delivery based on pH response.[204] Boronic acid, commonly used in crosslinking PVA hydrogels, forms reversible dynamic covalent bonds (boronate ester bonds) that confer self-healing properties to the polymer. These bonds, stable at pH < 8, can reversibly form or break depending on pH or aqueous media.[205] Exploiting such pH-dependent characteristics, crosslinked hydrogels using dispersion can be applied for pH responsiveness.[206] In one study, researchers crosslinked poly (aminobenzeneboronic acid)-cellulose nanocrystals and PVA chains through boron esterification to fabricate NIR light-induced self-healing and pH-responsive shape memory hydrogels. The results exhibited excellent mechanical strength along with high biocompatibility and shaped fixity and recovery rates (Figure 9bi–iii). In another study, a sensor hydrogel detecting

rapid resistance to deformation with excellent biocompatibility was produced by integrating CNCs-ABA (4-aminophenylboronic acid) and MWCNT into PVA. The conductivity of hydrogel was improved by the synergistic effect of MWCNT and NaOH.[166]

Light-responsive SMPs are based on dual-component materials incorporating polymer chains with glass transition temperatures ($T_g$) or melting temperatures ($T_m$) and photosensitive factors exhibiting sensitive light-responsive properties. Light-responsive SMPs are largely dominated by photoresponsive factors, which allow remote control, excellent focusing accuracy, and rapid transition. These factors are typically fabricated by grafting nanoparticles (NPs) onto the polymer via surface plasmon resonance.[207] Gold nanoparticles (AuNPs) endow the polymer with optically controllable shape memory and rapid optical healing properties due to uniform localized heating generated from surface plasmon resonance.[208] By grafting plasmonic silver nanoparticles (AgNPs) along CNC axes, rapid photothermal shape recovery properties under IR illumination are exhibited, along with synergy with the inherent antimicrobial properties of silver, enabling applications in smart biomedical materials (Figure 9ci–iii). Copper sulfide nanoparticles (CuSNPs) demonstrate excellent efficiency in phototriggered healing and shape memory properties through photothermal effects derived from copper ion d–d energy band transitions under NIR irradiation. It exhibits stability similar to AuNPs or carbon-based nanostructures and is much more economically accessible.[207,209]

### 5.3. Nanocellulose-Based Structural Color

Structural color is one of the types of luminescence that is commonly found in nature and is created by the way light waves strike the surface. Ordinary color displays create colors by using dyes or pigments that absorb some light wavelengths while letting others be reflected. In contrast, structural color, however, is produced by selective scattering, diffraction, and interference of light due to specific regular structures within its production medium. Structural color, when combined with soft hydrogels, can respond to dynamic stimuli, allowing color changes due to shape and volume changes. This enables primary color detection and secondary electrical response, making it possible to monitor as wearable sensors.[213] In one study, polymerized nonclose-packed colloidal arrays on GelMA and super-aligned carbon nanotube sheets (SACNTs) to create electrically conductive and anisotropic structural color hydrogels.[214] This hydrogel effectively induces the alignment of conductive cardiomyocytes. It contributes to the synchronous beating of myocardial cells, establishing a heart-on-a-chip system that visualizes the consistent beating rhythm through dynamic changes in structural color and reflective spectrum. In addition, changes in structural color due to dynamic stimuli can be used as a stimulus-responsive material. They can be utilized as light-responsive sensors for external stimuli such as temperature or NIR.[215]

Nanocellulose can also exhibit structural color like a film through self-assembly or microstructure formation.[216] A representative method for displaying structural color in nanocellulose is chiral nematic self-assembly.[217] The most common method involves extracting CNCs through sulfuric acid hydrolysis, where the crystals possess sulfate ester groups that give them a negative surface charge, allowing the formation of chiral nematic structures during the self-assembly of CNC colloidal solutions.[218] The helical chiral nematic structure is influenced by electrostatic repulsion and van der Waals forces acting on the nanocrystals. This structure can select photonic properties through a refractive index tunable based on physicochemical characteristics.[219] In one study, chiral nematic nanostructures were formed via evaporation-induced self-assembly of CNCs obtained through sulfuric acid hydrolysis, and fluorine ionic liquids (FILs) were added to create optical/electrical dual-signal sensing sensors with excellent water stability (**Figure 10a**). The introduction of hydrophobic FILs into CNC-based scaffold sensors showed positive results: strong thermal and chemical stability, low water absorption, and low surface energy. This indicates promise for applications in underwater detection and communication. Hydroxypropyl celluloses (HPCs), a cellulose derivative with hydroxypropyl substitution on the glucose unit, also exhibit a helical chiral nematic structure, which is further influenced by concentration, solvent effects, and dynamic principles (Figure 10bi,ii). In one study, produced ink with adjustable color saturation and rheological properties and capable of 3D printing was created by adding CNT and CNFs to HPCs (Figure 10cii). It was found that mixing with CNT decreased light transmittance but increased the saturation of reflected light, and while mixing with CNF did not affect the spontaneous formation of structural visible light, it showed a blueshift in the maximum reflection wavelength (Figure 10ci). This confirms the possibility of creating sensors that maintain structural color characteristics (Figure 10ciii,iv).

### 5.4. Nanocellulose-Based Nanogenerators and Electroluminescent Devices

Recently, beyond direct surface modification of cellulose, nanocellulose-based conductive hydrogels combined with various polymers have been researched, utilizing their unique molecular structures. For instance, triboelectric nanogenerators (TENGs) can convert irregular mechanical motions into electricity and thus represent a relatively new use for biobased polymers through contact/friction effects between all sorts of materials, attracting increasing interest as a novel energy source.[223] Cellulose, with its lightweight, low thermal expansion coefficient, excellent mechanical properties, and ideal micro/nano surface roughness, makes it an ideal material for active triboelectric materials in TENGs.[224] In addition, the high stretchability, antifreezing properties, and self-healing ability of hydrogels are highly attractive characteristics for TENGs that rely on contact/triboelectric effects.[225] The synergy between nanocellulose and hydrogels not only promotes crosslinking within the hydrogel and the formation of microchannels, enhancing the hydrogel's conductivity, but also increases triboelectric output through streaming potential[226] (**Figure 11ai–vi**). Another example of stretchable electroluminescent (EL) devices is a next-generation display technology capable of visually transmitting biosignals or electrical output under dynamic conditions, where conductive hydrogels are expected to play a significant role.[227] Nanocellulose-based hydrogels are very promising materials for applications in the field of EL devices

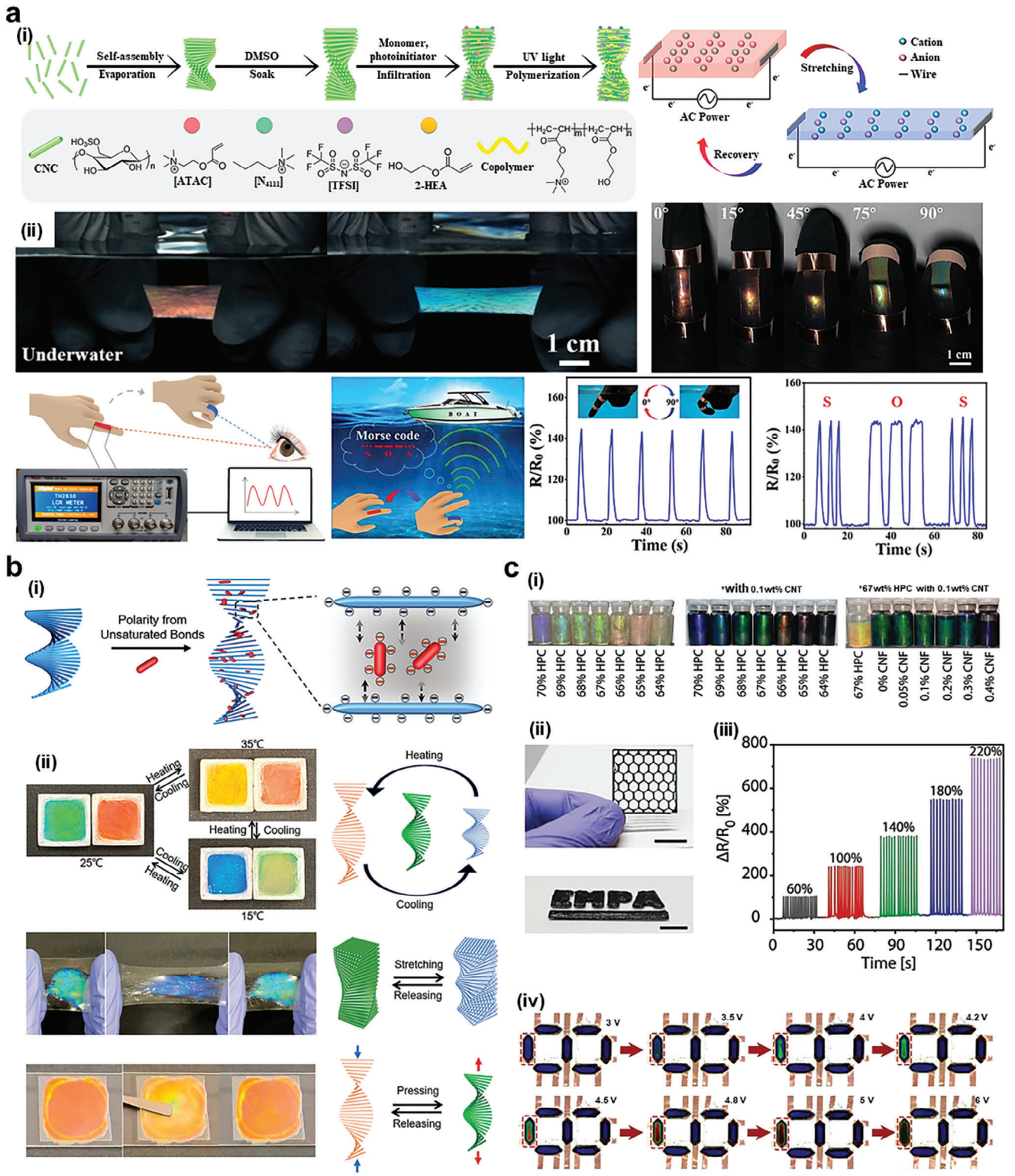


**Figure 10.** a) Noncontact sensing FILs–CNCs nanostructured film with excellent underwater stability.[220] Copyright 2023, American Chemical Society. i) Schematic of the synthesis and conduction mechanism of the FIL-CNC nanostructured film. ii) Structural color change and resistance variation (Morse code) due to dynamic stimuli underwater. b) Hydroxypropyl cellulose (HPC) matrix exhibiting a chiral nematic structure.[221] Copyright 2024, American Chemical Society. i) Schematic of the structural changes in the HPC gel. ii) Structural color change of the HPC gel in response to temperature, tension, and pressure. c) Multipurpose color-changing material: HPCs-CNT-CNFs printed composite materials.[222] Copyright 2023, Wiley-VCH. i) Saturation changes according to the content of CNT and CNFs. ii) 3D printed results of HPCs-CNT-CNFs. iii) Resistivity graph over time and strain. iv) Structural color change according to voltage.

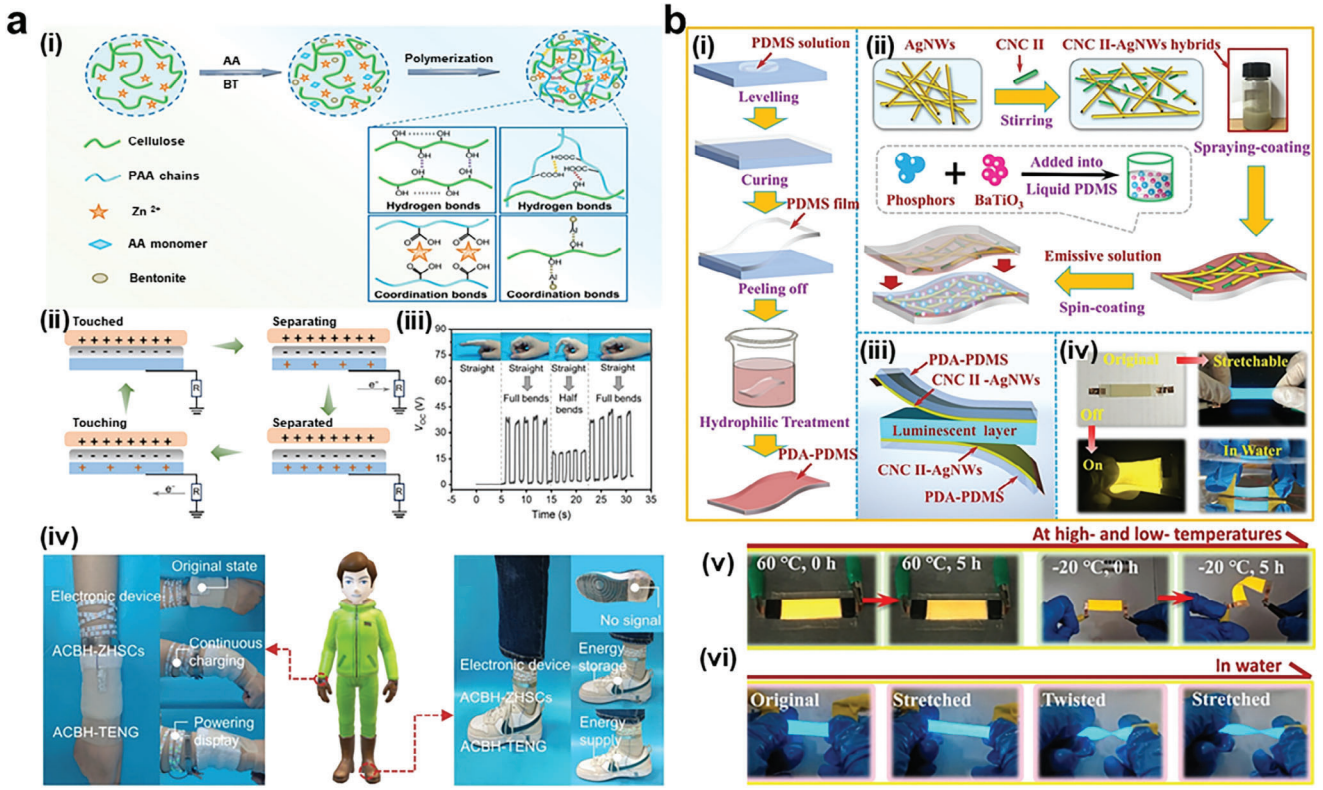


**Figure 11.** a) Nanocellulose hydrogel-based TENGs.[230] Copyright 2024, Elsevier Ltd. i) Schematics diagram of the hydrogel-based TENGs. ii) Mechanism of the hydrogel-based TENGs. iii) TENGs' performance of finger bending detection. iv) Demonstration picture of TENGs powering an electrical appliance. b) Nanocellulose hydrogel-based EL device.[231] Copyright 2022, Elsevier Ltd. i) Schematic diagram of the hydrophilic polydimethylsiloxane surface preparation. ii) Schematic diagram of flexible EL device. iii) Schematic diagram of the structure of the EL device. iv) Image of the EL device in OFF/ON states, under stretching and in water. v) Image of EL devices working at −20 and 60 °C for 5 h. vi) Image of EL devices stretching and twisting underwater.

because of their environmental resistance, good stretchability, stability in mechanical cycling, and self-adhesion properties[228] (Figure 11bi–v). The properties of EL devices make them suitable for "E-skin," which is an indication of the growing applicability of nanocellulose-based hydrogels in wearable devices.[229]

Based on the properties of nanocellulose and other materials discussed in the abovementioned sections, **Table 5** summarizes a comparative study highlighting the advantages and disadvantages of nanocellulose-based hydrogel compared to the other materials, along with their applications.

## 6. Summary and Future Prospects

In this review, we discuss the basic types of nanocellulose and present in detail the intrinsic properties and manufacturing techniques of nanocellulose-based hydrogels. Nanocellulose is a natural polymer with a uniform repeating structure containing a large number of hydroxyl groups, which becomes an attractive material with unlimited application prospects by incorporating or modifying these hydroxyl groups. Nanocellulose-based hydrogels improve the mechanical properties of traditional hydrogels and possess excellent mechanical and rheological properties as well as biocompatibility, making them promising materials in various fields, especially for applications in the human body, such as tissue engineering and biomedical fields. Hydrogels are also tunable materials that can easily achieve desired outcomes by altering interactions and relative quantification of the material. Furthermore, the incorporation of conductive structures into these hydrogels with methods such as conductive polymers, carbon types of material, and carbon dots has been found to greatly improve the utility of the hydrogels in electronics and biomedical applications. Advanced fabrication techniques, especially various 3D printing processes and gel strategies, have proven to be essential in developing nanocellulose-based hydrogels with customized structures and functions.

However, to use nanocellulose in hydrogels, surface modification is required to disperse it in a solvent. This process should be done carefully since other poisonous substances may be used in this process, which will be a threat to the biocompatibility feature of nanocellulose. Furthermore, the processes involving nanocellulose-based hydrogel production, especially those concerning constant quality and uniformity of the synthesized hydrogels, create practical concerns about the cost-effectiveness of large-scale production of nanocellulose-based hydrogels and their synthesis and environmental impacts. The modification process needs to be carefully considered and optimized. In addition, ensuring the long-term stability and durability of these hydrogels under various environmental conditions is crucial for

**Table 5.** Comparison of polymeric hydrogels with and without nanocellulose for various tissue engineering applications.

| Polymer composites | Properties | Without nanocellulose | With nanocellulose | Applications | References |
|---|---|---|---|---|---|
| Sodium alginate/ polyacrylamide/CNC | Adsorption capabilities | Regular adsorption ability for basic application | Enhanced adsorption property due to increased surface area | Drug delivery | [232] |
| | Thermal stability | Limited thermal stability | Enhanced thermal stability | Cancer treatment | [232a, 233] |
| Tannic acid-modified 2,2,6,6-tetramethylpiperidin-1-yloxy-oxidized cellulose nanofibers and MXene | Mechanical strength | Reduced or average mechanical strength | High mechanical strength | Photoelectronic devices, wearable sensors | [155a, 234] |
| | Degradation stability | Rapid degradation rate | Highly stable and slow degradation rate due to hydrogen and ionic bonding | Wound healing, antibacterial flexible sensors | [234,235] |
| | Biocompatibility | Reduced biocompatibility due to MXenes incorporation | Increased biocompatibility | Electronic skin sensors | [234, 236] |
| Silver nanowire-CNC/ crystalline allomorph/ polydimethylsiloxane | Elasticity | Regular elasticity | Highly stretchable | Electroluminescent devices | [228a] |
| | Self-adhesiveness | Reduced adhesiveness | Highly self-adhesive | Wound healing, motion-detecting sensors | [228a, 237] |
| Cellulose composite gels | Crystallinity | Lower crystallinity | Improved crystallinity | Drug delivery, cartilage regeneration | [238] |
| | Gelation | Standard gelation rate | Increased/ accelerated gelation | Wound healing | [238a] |
| | Thermal stability | Decreased thermal stability | Increased thermal stability | Drug delivery | [237–239] |
| Polypyrrole/prussian blue/CNC | Water retention | Low water retention rate | High water content | Vascular graft preparation | [240] |
| | Electrical conductivity | Limited conductivity | Enhanced electrical conductivity | Wound healing | [241] |
| | pH sensitivity | Decreased sensitivity to pH | Highly sensitive to pH change | – | [241] |

their practical application. In addition, while introducing conductive elements into nanocellulose hydrogels can improve their functionality, it is also important to clearly understand the interaction mechanisms at the molecular level. It will aid in the fine-tuning of hydrogels for certain applications, including bioelectronics, where the conductivity of hydrogels and mechanical strength are imperative, or for future soft robots.

In conclusion, the constant development investigations on tunable nanocellulose-based conductive hydrogels are considered of great interest. Suppose further research and development are invested in these hydrogels. In that case, they will be expected to significantly impact various industries by providing long-lasting, high-performance solutions to a variety of problems. The future nanocellulose-based hydrogels are indeed exciting, with bright potential, practical applications, and sustainability. These solutions are suitable for a variety of complex problems and applications.

## Acknowledgements

M.J.J. and A.R. contributed equally to this work. This study was supported by the "Basic Science Research Program" through the "National Research Foundation of Korea" funded by the "Ministry of Education" (NRF2022R1I1A3063302 and NRF2018R1A6A1A03025582). This work was also supported by Innovative Human Resource Development for Local Intellectualization program through the Institute of Information and Communications Technology Planning and Evaluation (IITP) grant funded by the Korean government (MSIT) (IITP-2024-RS-2023-00260267).

## Conflict of Interest

The authors declare no conflict of interest.

## Keywords

3D-printing, biomedical engineering, conductive hydrogel, nanocellulose, tunable hydrogel

Received: November 4, 2024
Revised: November 18, 2024
Published online:

[1] a) K. Mo, T. Zhang, W. Yan, C. Chang, *Cellulose* **2018**, *25*, 6561; b) Y. Zheng, L. Zhang, B. Duan, *Carbohydr. Polym.* **2022**, *295*, 119866.
[2] a) Y. J. Wang, X. N. Zhang, Y. Song, Y. Zhao, L. Chen, F. Su, L. Li, Z. L. Wu, Q. Zheng, *Chem. Mater.* **2019**, *31*, 1430; b) H. Yu, N. Rouelle, A. Qiu, J.-A. Oh, D. M. Kempaiah, J. D. Whittle, M. Aakyiir, W. Xing, J. Ma, *ACS Appl. Mater. Interfaces* **2020**, *12*, 37977.
[3] a) S. Liu, O. Oderinde, I. Hussain, F. Yao, G. Fu, *Polymer* **2018**, *144*, 111; b) J. Yin, S. Pan, L. Wu, L. Tan, D. Chen, S. Huang, Y. Zhang, P. He, *J. Mater. Chem. C* **2020**, *8*, 17349.
[4] a) Z. Ren, T. Ke, Q. Ling, L. Zhao, H. Gu, *Carbohydr. Polym.* **2021**, *273*, 118533; b) Y. Liang, Z. Li, Y. Huang, R. Yu, B. Guo, *ACS Nano* **2021**, *15*, 7078.
[5] a) M. P. Sekar, S. Suresh, A. Zennifer, S. Sethuraman, D. Sundaramurthi, *ACS Biomater. Sci. Eng.* **2023**, *9*, 3134; b) K. Teng, Q. An, Y. Chen, Y. Zhang, Y. Zhao, *ACS Biomater. Sci. Eng.* **2021**, *7*,

1302; c) M. Rajabi, M. McConnell, J. Cabral, M. A. Ali, *Carbohydr. Polym.* **2021**, *260*, 117768.
[6] a) Y. Wang, Z. Wang, Y. Dong, *ACS Biomater. Sci. Eng.* **2023**, *9*, 1132; b) S. Mohanto, S. Narayana, K. P. Merai, J. A. Kumar, A. Bhunia, U. Hani, A. Al Fatease, B. J. Gowda, S. Nag, M. G. Ahmed, *Int. J. Biol. Macromol.* **2023**, *253*, 127143.
[7] F. Li, J. Tang, J. Geng, D. Luo, D. Yang, *Prog. Polym. Sci.* **2019**, *98*, 101163.
[8] C. Xu, G. Dai, Y. Hong, *Acta Biomater.* **2019**, *95*, 50.
[9] a) P. Heidarian, S. Gharaie, H. Yousefi, M. Paulino, A. Kaynak, R. Varley, A. Z. Kouzani, *Carbohydr. Polym.* **2022**, *291*, 119545; b) O. Fourmann, M. K. Hausmann, A. Neels, M. Schubert, G. Nyström, T. Zimmermann, G. Siqueira, *Carbohydr. Polym.* **2021**, *259*, 117716; c) C. Sun, Y. Xie, H. Zhu, X. Zheng, R. Hou, Z. Shi, J. Li, Q. Yang, *Biomacromolecules* **2023**, *24*, 5989.
[10] a) K. Dhali, M. Ghasemlou, F. Daver, P. Cass, B. Adhikari, *Sci. Total Environ.* **2021**, *775*, 145871; b) W. Perdoch, Z. Cao, P. Florczak, R. Markiewicz, M. Jarek, K. Olejnik, B. Mazela, *Molecules* **2022**, *27*, 4696.
[11] X. He, Q. Lu, *Carbohydr. Polym.* **2023**, *301*, 120351.
[12] H. Liu, K. Liu, X. Han, H. Xie, C. Si, W. Liu, Y. Bae, *Curr. Med. Chem.* **2020**, *27*, 4622.
[13] F. Barja, *J. Biomed. Res.* **2021**, *35*, 310.
[14] a) X.-R. Ong, A. X. Chen, N. Li, Y. Y. Yang, H.-K. Luo, *Small Sci.* **2023**, *3*, 2200076; b) V. Thakur, A. Guleria, S. Kumar, S. Sharma, K. Singh, *Mater. Adv.* **2021**, *2*, 1872.
[15] Y. Wu, Y. Liang, C. Mei, L. Cai, A. Nadda, Q. Van Le, Y. Peng, S. S. Lam, C. Sonne, C. Xia, *Chemosphere* **2022**, *286*, 131891.
[16] Y. Huo, Y. Liu, M. Xia, H. Du, Z. Lin, B. Li, H. Liu, *Polymers* **2022**, *14*, 2648.
[17] K. Heise, E. Kontturi, Y. Allahverdiyeva, T. Tammelin, M. B. Linder, O. I. Nonappa, *Adv. Mater.* **2021**, *33*, 2004349.
[18] H. Baniasadi, E. Kimiaei, R. T. Polez, R. Ajdary, O. J. Rojas, M. Österberg, J. Seppälä, *Int. J. Biol. Macromol.* **2022**, *209*, 2020.
[19] X. Yang, S. K. Biswas, J. Han, S. Tanpichai, M. C. Li, C. Chen, S. Zhu, A. K. Das, H. Yano, *Adv. Mater.* **2021**, *33*, 2002264.
[20] W. D. Callister Jr, D. G. Rethwisch, *Materials Science and Engineering: An Introduction*, John Wiley and Sons, Hoboken, NJ, USA **2020**.
[21] J.-B. Yan, J. R. Liew, M.-H. Zhang, J.-Y. Wang, *Mater. Des.* **2014**, *61*, 150.
[22] F. Hussain, M. Hojjati, M. Okamoto, R. E. Gorga, *J. Compos. Mater.* **2006**, *40*, 1511.
[23] J.-P. Salvetat, S. Bhattacharyya, R. B. Pipes, *J. Nanosci. Nanotechnol.* **2006**, *6*, 1857.
[24] T. Nishino, R. Matsui, K. Nakamae, *J. Polym. Sci., Part B: Polym. Phys.* **1999**, *37*, 1191.
[25] R. Hori, M. Wada, *Cellulose* **2005**, *12*, 479.
[26] a) J. Ma, J. Zhong, F. Sun, B. Liu, Z. Peng, J. Lian, X. Wu, L. Li, M. Hao, T. Zhang, *Chem. Eng. J.* **2023**, *481*, 148317; b) J. Gamboa, S. Paulo-Mirasol, F. Estrany, J. Torras, *ACS Appl. Bio Mater.* **2023**, *6*, 1720.
[27] a) G. Thrivikraman, S. K. Boda, B. Basu, *Biomaterials* **2018**, *150*, 60; b) B. Yang, C. Liang, D. Chen, F. Cheng, Y. Zhang, S. Wang, J. Shu, X. Huang, J. Wang, K. Xia, *Bioact. Mater.* **2022**, *15*, 103; c) Z. M. Khan, E. Wilts, E. Vlaisavljevich, T. E. Long, S. S. Verbridge, *Macromol. Biosci.* **2022**, *22*, 2100355.
[28] Z. Shi, X. Gao, M. W. Ullah, S. Li, Q. Wang, G. Yang, *Biomaterials* **2016**, *111*, 40.
[29] Q. Yang, M. He, Z. Yu, Y. Liu, Y. Bai, T. Liu, T. Wang, L. Meng, F. Meng, Q. Ma, *Chem. Eng. J.* **2024**, *495*, 153567.
[30] X. Wang, Q. Wang, C. Xu, *Bioengineering* **2020**, *7*, 40.
[31] J. Su, L. Zhang, C. Wan, Z. Deng, S. Wei, K.-T. Yong, Y. Wu, *Carbohydr. Polym.* **2022**, *296*, 119905.
[32] R. Ramachandran, D. Jung, A. M. Spokoyny, *NPG Asia Mater.* **2019**, *11*, 19.
[33] Z. Wang, F. Cheng, H. Cai, X. Li, J. Sun, Y. Wu, N. Wang, Y. Zhu, *Carbohydr. Polym.* **2021**, *259*, 117753.
[34] D. Ye, S. Rongpipi, S. N. Kiemle, W. J. Barnes, A. M. Chaves, C. Zhu, V. A. Norman, A. Liebman-Peláez, A. Hexemer, M. F. Toney, *Nat. Commun.* **2020**, *11*, 4720.
[35] H. Khanjanzadeh, R. Behrooz, N. Bahramifar, W. Gindl-Altmutter, M. Bacher, M. Edler, T. Griesser, *Int. J. Biol. Macromol.* **2018**, *106*, 1288.
[36] J. Xu, Z. Wu, Q. Wu, Y. Kuang, *Carbohydr. Polym.* **2020**, *229*, 115553.
[37] L. Gan, J. Liao, N. Lin, C. Hu, H. Wang, J. Huang, *ACS Omega* **2017**, *2*, 4725.
[38] J. Guo, W. Du, Y. Gao, Y. Cao, Y. Yin, *Colloids Surf. A* **2017**, *529*, 634.
[39] N. M. Girouard, S. Xu, G. T. Schueneman, M. L. Shofner, J. C. Meredith, *ACS Appl. Mater. Interfaces* **2016**, *8*, 1458.
[40] M. Cheng, Z. Qin, J. Hu, Q. Liu, T. Wei, W. Li, Y. Ling, B. Liu, *Carbohydr. Polym.* **2020**, *231*, 115701.
[41] L. Ning, C. You, Y. Zhang, X. Li, F. Wang, *Life Sci.* **2020**, *241*, 117137.
[42] Y. Noguchi, I. Homma, Y. Matsubara, *Cellulose* **2017**, *24*, 1295.
[43] J. A. Sirviö, M. Visanko, H. Liimatainen, *Green Chem.* **2015**, *17*, 3401.
[44] H. Liimatainen, M. Visanko, J. A. Sirvio, O. E. Hormi, J. Niinimaki, *Biomacromolecules* **2012**, *13*, 1592.
[45] Y. Lee, H. Zhang, H.-Y. Yu, K. C. Tam, *Carbohydr. Polym.* **2022**, *289*, 119419.
[46] I. B. Tabar, X. Zhang, J. P. Youngblood, N. S. Mosier, *Carbohydr. Polym.* **2017**, *174*, 120.
[47] M. S. M. Misenan, Z. Akhlisah, A. Shaffie, M. A. M. Saad, M. Norrrahim, Industrial Applications of Nanocellulose and Its Nanocomposites, Elsevier, Amsterdam, Netherlands **2022**, p. 213.
[48] B. Alonso-Lerma, L. Barandiaran, L. Ugarte, I. Larraza, A. Reifs, R. Olmos-Juste, N. Barruetabeña, I. Amenabar, R. Hillenbrand, A. Eceiza, *Commun. Mater.* **2020**, *1*, 57.
[49] C. L. Pirich, G. F. Picheth, J. P. E. Machado, C. N. Sakakibara, A. A. Martin, R. A. de Freitas, M. R. Sierakowski, *Int. J. Biol. Macromol.* **2019**, *130*, 622.
[50] a) H. Wang, H. Xie, H. Du, X. Wang, W. Liu, Y. Duan, X. Zhang, L. Sun, X. Zhang, C. Si, *Carbohydr. Polym.* **2020**, *239*, 116233; b) O. M. Vanderfleet, M. S. Reid, J. Bras, L. Heux, J. Godoy-Vargas, M. K. Panga, E. D. Cranston, *Cellulose* **2019**, *26*, 507.
[51] L. Xing, J. Gu, W. Zhang, D. Tu, C. Hu, *Carbohydr. Polym.* **2018**, *192*, 184.
[52] J. M. Yarbrough, R. Zhang, A. Mittal, T. Vander Wall, Y. J. Bomble, S. R. Decker, M. E. Himmel, P. N. Ciesielski, *ACS Nano* **2017**, *11*, 3101.
[53] O. M. Vanderfleet, E. D. Cranston, *Nat. Rev. Mater.* **2021**, *6*, 124.
[54] S. P. Bangar, M. Harussani, R. Ilyas, A. O. Ashogbon, A. Singh, M. Trif, S. M. Jafari, *Food Hydrocolloids* **2022**, *130*, 107689.
[55] T. Aziz, H. Fan, X. Zhang, F. Haq, A. Ullah, R. Ullah, F. U. Khan, M. Iqbal, *J. Polym. Environ.* **2020**, *28*, 1117.
[56] a) J. Li, D. J. Mooney, *Nat. Rev. Mater.* **2016**, *1*, 1; b) A. C. M. Cidreira, K. C. de Castro, T. Hatami, L. Z. Linan, L. H. I. Mei, *Biomed. Microdevices* **2021**, *23*, 43.
[57] a) W. Chen, H. Yu, Y. Liu, P. Chen, M. Zhang, Y. Hai, *Carbohydr. Polym.* **2011**, *83*, 1804; b) R. Kose, I. Mitani, W. Kasai, T. Kondo, *Biomacromolecules* **2011**, *12*, 716.
[58] a) X. Han, R. Bi, V. Khatri, H. Oguzlu, M. Takada, J. Jiang, F. Jiang, J. Bao, J. N. Saddler, *ACS Sustainable Chem. Eng.* **2021**, *9*, 1406; b) X. Han, R. Bi, H. Oguzlu, M. Takada, J. Jiang, F. Jiang, J. Bao, J. N. Saddler, *ACS Sustainable Chem. Eng.* **2020**, *8*, 14955.
[59] a) X. Yang, L. Li, Y. Nishiyama, M. S. Reid, L. A. Berglund, *Carbohydr. Polym.* **2023**, *312*, 120788; b) F. Hoeng, A. Denneulin, J. Bras, *Nanoscale* **2016**, *8*, 13131.
[60] M. Asyraf, M. Rafidah, A. Azrina, M. Razman, *Cellulose* **2021**, *28*, 2675.

[61] a) A. Isogai, T. Saito, H. Fukuzumi, *Nanoscale* **2011**, *3*, 71; b) Z. Tang, X. Lin, M. Yu, A. K. Mondal, H. Wu, *Int. J. Biol. Macromol.* **2023**, *259*, 129081.
[62] I. Besbes, S. Alila, S. Boufi, *Carbohydr. Polym.* **2011**, *84*, 975.
[63] T. Saito, A. Isogai, *Colloids Surf. A* **2006**, *289*, 219.
[64] Z. Zai, M. Yan, C. Shi, L. Zhang, H. Lu, Z. Xiong, J. Ma, *Int. J. Biol. Macromol.* **2022**, *207*, 23.
[65] a) F. Kimura, T. Kimura, M. Tamura, A. Hirai, M. Ikuno, F. Horii, *Langmuir* **2005**, *21*, 2034; b) H. C. Kim, J. W. Kim, L. Zhai, J. Kim, *Cellulose* **2019**, *26*, 5821.
[66] a) D. Bordel, J.-L. Putaux, L. Heux, *Langmuir* **2006**, *22*, 4899; b) A. Kadimi, K. Benhamou, Z. Ounaies, A. Magnin, A. Dufresne, H. Kaddami, M. Raihane, *ACS Appl. Mater. Interfaces* **2014**, *6*, 9418.
[67] a) K. Li, C. M. Clarkson, L. Wang, Y. Liu, M. Lamm, Z. Pang, Y. Zhou, J. Qian, M. Tajvidi, D. J. Gardner, *ACS Nano* **2021**, *15*, 3646; b) A. Kafy, H. C. Kim, L. Zhai, J. W. Kim, L. V. Hai, T. J. Kang, J. Kim, *Sci. Rep.* **2017**, *7*, 17683.
[68] a) I. Reiniati, A. N. Hrymak, A. Margaritis, *Biochem. Eng. J.* **2017**, *127*, 21; b) C. Sharma, N. K. Bhardwaj, *Int. J. Biol. Macromol.* **2019**, *132*, 166.
[69] a) P. Jacek, F. A. S. da Silva, F. Dourado, S. Bielecki, M. Gama, *Carbohydr. Polym. Technol. Applications* **2021**, *2*, 100022; b) D. Abol-Fotouh, M. A. Hassan, H. Shokry, A. Roig, M. S. Azab, A. E.-H. B. Kashyout, *Sci. Rep.* **2020**, *10*, 3491.
[70] M. Foresti, P. Cerrutti, A. Vazquez, Polymer Nanocomposites Based on Inorganic and Organic Nanomaterials, Scrivener Publishing LLC, Beverly, Massachusetts, USA **2015**, p. 39.
[71] W. Y. Bang, O. E. Adedeji, H. J. Kang, M. D. Kang, J. Yang, Y. W. Lim, Y. H. Jung, *Int. J. Biol. Macromol.* **2021**, *193*, 269.
[72] a) H. Khan, V. Saroha, S. Raghuvanshi, A. K. Bharti, D. Dutt, *Carbohydr. Polym.* **2021**, *260*, 117807; b) A. C. Lee, M. M. Salleh, M. F. Ibrahim, E. K. Bahrin, M. A. Jenol, S. Abd-Aziz, *Biomass Convers. Biorefin.* **2024**, *14*, 5541.
[73] H. Gao, Q. Sun, Z. Han, J. Li, B. Liao, L. Hu, J. Huang, C. Zou, C. Jia, J. Huang, *Carbohydr. Polym.* **2020**, *227*, 115323.
[74] K. Yu, S. Balasubramanian, H. Pahlavani, M. J. Mirzaali, A. A. Zadpoor, M.-E. Aubin-Tam, *ACS Appl. Mater. Interfaces* **2020**, *12*, 50748.
[75] H. Kim, S. D. Dutta, A. Randhawa, T. V. Patil, K. Ganguly, R. Acharya, J. Lee, H. Park, K.-T. Lim, *Int. J. Biol. Macromol.* **2024**, *264*, 130732.
[76] a) C. Ruan, Y. Zhu, X. Zhou, N. Abidi, Y. Hu, J. M. Catchmark, *Cellulose* **2016**, *23*, 3417; b) A. F. Jozala, L. C. de Lencastre-Novaes, A. M. Lopes, V. de Carvalho Santos-Ebinuma, P. G. Mazzola, A. Pessoa-Jr, D. Grotto, M. Gerenutti, M. V. Chaud, *Appl. Microbiol. Biotechnol.* **2016**, *100*, 2063.
[77] R. Ajdary, B. L. Tardy, B. D. Mattos, L. Bai, O. J. Rojas, *Adv. Mater.* **2021**, *33*, 2001085.
[78] a) C. Zhu, T. Y.-J. Han, E. B. Duoss, A. M. Golobic, J. D. Kuntz, C. M. Spadaccini, M. A. Worsley, *Nat. Commun.* **2015**, *6*, 6962; b) L. R. Meza, S. Das, J. R. Greer, *Science* **2014**, *345*, 1322.
[79] C.-W. Lai, S.-S. Yu, *ACS Appl. Mater. Interfaces* **2020**, *12*, 34235.
[80] J. Jiang, H. Oguzlu, F. Jiang, *Chem. Eng. J.* **2021**, *405*, 126668.
[81] Y. Li, H. Zhu, Y. Wang, U. Ray, S. Zhu, J. Dai, C. Chen, K. Fu, S. H. Jang, D. Henderson, *Small Methods* **2017**, *1*, 1700222.
[82] V. K. Vorobiov, M. P. Sokolova, N. V. Bobrova, V. Y. Elokhovsky, M. A. Smirnov, *Carbohydr. Polym.* **2022**, *290*, 119475.
[83] K. Maity, A. Mondal, M. C. Saha, *ACS Appl. Mater. Interfaces* **2023**, *15*, 13956.
[84] Z. Guo, C. Ma, W. Xie, A. Tang, W. Liu, *Carbohydr. Polym.* **2023**, *315*, 121006.
[85] S. D. Dutta, T. V. Patil, K. Ganguly, A. Randhawa, R. Acharya, M. Moniruzzaman, K.-T. Lim, *Carbohydr. Polym.* **2023**, *320*, 121232.
[86] X. Cui, J. Li, Y. Hartanto, M. Durham, J. Tang, H. Zhang, G. Hooper, K. Lim, T. Woodfield, *Adv. Healthcare Mater.* **2020**, *9*, 1901648.
[87] G. Percoco, L. Arleo, G. Stano, F. Bottiglione, *Addit. Manuf.* **2021**, *38*, 101791.
[88] a) B. C. Palivela, S. D. Bandari, R. S. Mamilla, *Bioprinting* **2022**, *27*, e00219; b) N. Putra, M. Leeflang, P. Taheri, L. Fratila-Apachitei, J. Mol, J. Zhou, A. Zadpoor, *Acta Biomater.* **2021**, *134*, 774.
[89] G. Falcone, P. Mazzei, A. Piccolo, T. Esposito, T. Mencherini, R. P. Aquino, P. Del Gaudio, P. Russo, *Carbohydr. Polym.* **2022**, *276*, 118746.
[90] S. Bom, R. Ribeiro, H. M. Ribeiro, C. Santos, J. Marto, *Int. J. Pharm.* **2022**, *615*, 121506.
[91] P. Amorim, M. d'Ávila, R. Anand, P. Moldenaers, P. Van Puyvelde, V. Bloemen, *Bioprinting* **2021**, *22*, e00129.
[92] T. Ma, L. Lv, C. Ouyang, X. Hu, X. Liao, Y. Song, X. Hu, *Carbohydr. Polym.* **2021**, *253*, 117217.
[93] W. Xu, B. Z. Molino, F. Cheng, P. J. Molino, Z. Yue, D. Su, X. Wang, S. Willför, C. Xu, G. G. Wallace, *ACS Appl. Mater. Interfaces* **2019**, *11*, 8838.
[94] a) M. Latif, Y. Jiang, B. Kumar, H. C. Cho, J. M. Song, J. Kim, *ACS Appl. Nano Mater.* **2022**, *5*, 5680; b) M. K. Hausmann, G. Siqueira, R. Libanori, D. Kokkinis, A. Neels, T. Zimmermann, A. R. Studart, *Adv. Funct. Mater.* **2020**, *30*, 1904127.
[95] M. Latif, Y. Jiang, J. Kim, *Carbohydr. Polym.* **2023**, *320*, 121197.
[96] a) S. H. Kim, Y. K. Yeon, J. M. Lee, J. R. Chao, Y. J. Lee, Y. B. Seo, M. T. Sultan, O. J. Lee, J. S. Lee, S.-i. Yoon, *Nat. Commun.* **2018**, *9*, 1620; b) D. Xue, J. Zhang, Y. Wang, D. Mei, *ACS Biomater. Sci. Eng.* **2019**, *5*, 4825.
[97] H. Wang, B. Zhang, J. Zhang, X. He, F. Liu, J. Cui, Z. Lu, G. Hu, J. Yang, Z. Zhou, *ACS Appl. Mater. Interfaces* **2021**, *13*, 55507.
[98] a) J. Yao, M. Hakkarainen, *Compos. Commun.* **2023**, *38*, 101506; b) L. Yue, S. M Montgomery, X. Sun, L. Yu, Y. Song, T. Nomura, M. Tanaka, H. J Qi, *Nat. Commun.* **2023**, *14*, 1251; c) L. Wang, F. Zhang, Y. Liu, S. Du, J. Leng, *ACS Appl. Mater. Interfaces* **2021**, *13*, 18110.
[99] a) G. Zhu, M. Liu, Z. Kou, G. Zhang, C. Bo, L. Hu, Y. Hu, Y. Zhou, *Chem. Eng. J.* **2023**, *475*, 146080; b) G. Zhu, Y. Hou, J. Xiang, J. Xu, N. Zhao, *ACS Appl. Mater. Interfaces* **2021**, *13*, 34954; c) G. Zhu, J. Zhang, J. Huang, Y. Qiu, M. Liu, J. Yu, C. Liu, Q. Shang, Y. Hu, L. Hu, *Chem. Eng. J.* **2023**, *452*, 139401.
[100] a) G. Siqueira, D. Kokkinis, R. Libanori, M. K. Hausmann, A. S. Gladman, A. Neels, P. Tingaut, T. Zimmermann, J. A. Lewis, A. R. Studart, *Adv. Funct. Mater.* **2017**, *27*, 1604619; b) M. Maturi, C. Spanu, N. Fernández-Delgado, S. I. Molina, M. C. Franchini, E. Locatelli, A. S. de León, *Addit. Manuf.* **2023**, *61*, 103342.
[101] V. C.-F. Li, X. Kuang, A. Mulyadi, C. M. Hamel, Y. Deng, H. J. Qi, *Cellulose* **2019**, *26*, 3973.
[102] a) S. Mallakpour, M. Tukhani, C. M. Hussain, *Adv. Colloid Interface Sci.* **2021**, *292*, 102415; b) X. Wang, J. Qi, W. Zhang, Y. Pu, R. Yang, P. Wang, S. Liu, X. Tan, B. Chi, *Int. J. Biol. Macromol.* **2021**, *187*, 91; c) D. Cafiso, A. A. Septevani, C. Noè, T. Schiller, C. F. Pirri, I. Roppolo, A. Chiappone, *Sustainable Mater. Technol.* **2022**, *32*, e00444.
[103] J. Lee, S. D. Dutta, R. Acharya, H. Park, H. Kim, A. Randhawa, T. V. Patil, K. Ganguly, R. Luthfikasari, K. T. Lim, *Adv. Healthcare Mater.* **2024**, *13*, 2302394.
[104] J. Wang, A. Goyanes, S. Gaisford, A. W. Basit, *Int. J. Pharm.* **2016**, *503*, 207.
[105] R. Palucci Rosa, G. Rosace, *Macromol. Mater. Eng.* **2021**, *306*, 2100345.
[106] K. M. Håkansson, I. C. Henriksson, C. de la Peña Vázquez, V. Kuzmenko, K. Markstedt, P. Enoksson, P. Gatenholm, *Adv. Mater. Technol.* **2016**, *1*, 1600096.
[107] S. Shin, H. Kwak, D. Shin, J. Hyun, *Nat. Commun.* **2019**, *10*, 4650.
[108] Y. Chen, Z. Yu, Y. Ye, Y. Zhang, G. Li, F. Jiang, *ACS Nano* **2021**, *15*, 1869.
[109] a) W. Hu, Z. Wang, Y. Xiao, S. Zhang, J. Wang, *Biomater. Sci.* **2019**, *7*, 843; b) M. Hoque, M. Alam, S. Wang, J. U. Zaman, M. S. Rahman,

M. Johir, L. Tian, J.-G. Choi, M. B. Ahmed, M.-H. Yoon, *Mater. Sci. Eng., R* **2023**, *156*, 100758.
[110] a) M. Zhang, X. Zhao, *Int. J. Biol. Macromol.* **2020**, *162*, 1414; b) Y. Yang, D. Wu, *Chin. J. Chem.* **2022**, *40*, 2118.
[111] J. Shen, Y. Dai, F. Xia, X. Zhang, *Prog. Polym. Sci.* **2022**, *135*, 101622.
[112] J. Y. Seo, B. Lee, T. W. Kang, J. H. Noh, M. J. Kim, Y. B. Ji, H. J. Ju, B. H. Min, M. S. Kim, *Tissue Eng. Regener. Med.* **2018**, *15*, 513.
[113] a) Z. Li, B. H. Tan, *Mater. Sci. Eng., C* **2014**, *45*, 620; b) W. Wang, Y. Zhang, W. Liu, *Prog. Polym. Sci.* **2017**, *71*, 1.
[114] Y. Zhang, M. Song, Y. Diao, B. Li, L. Shi, R. Ran, *RSC Adv.* **2016**, *6*, 112468.
[115] X. Li, C. Wan, T. Tao, H. Chai, Q. Huang, Y. Chai, Y. Wu, *Cellulose* **2024**, *31*, 61.
[116] D. Hu, M. Zeng, Y. Sun, J. Yuan, Y. Wei, *SusMat* **2021**, *1*, 266.
[117] Y. Deng, I. Hussain, M. Kang, K. Li, F. Yao, S. Liu, G. Fu, *Chem. Eng. J.* **2018**, *353*, 900.
[118] a) X. Chang, Y. Geng, H. Cao, J. Zhou, Y. Tian, G. Shan, Y. Bao, Z. L. Wu, P. Pan, *Macromol. Rapid Commun.* **2018**, *39*, 1700806; b) X. N. Zhang, Y. J. Wang, S. Sun, L. Hou, P. Wu, Z. L. Wu, Q. Zheng, *Macromolecules* **2018**, *51*, 8136; c) J. Pan, Y. Jin, S. Lai, L. Shi, W. Fan, Y. Shen, *Chem. Eng. J.* **2019**, *370*, 1228.
[119] W. E. Hennink, C. F. van Nostrum, *Adv. Drug Delivery Rev.* **2012**, *64*, 223.
[120] a) X.-H. Wang, F. Song, D. Qian, Y.-D. He, W.-C. Nie, X.-L. Wang, Y.-Z. Wang, *Chem. Eng. J.* **2018**, *349*, 588; b) X. Li, Q. Yang, Y. Zhao, S. Long, J. Zheng, *Soft Matter* **2017**, *13*, 911; c) H. Chen, Y. Liu, B. Ren, Y. Zhang, J. Ma, L. Xu, Q. Chen, J. Zheng, *Adv. Funct. Mater.* **2017**, *27*, 1703086.
[121] Y. Lin, H. Zhang, H. Liao, Y. Zhao, K. Li, *Chem. Eng. J.* **2019**, *367*, 139.
[122] a) J. Niu, J. Wang, X. Dai, Z. Shao, X. Huang, *Carbohydr. Polym.* **2018**, *193*, 73; b) C. Castro, R. Zuluaga, O. Rojas, I. Filpponen, H. Orelma, M. Londoño, S. Betancourt, P. Gañán, *RSC Adv.* **2015**, *5*, 90742.
[123] a) A. Morales, J. Labidi, P. Gullón, *J. Ind. Eng. Chem.* **2020**, *81*, 475; b) A. Morales, J. Labidi, P. Gullón, *Sustainable Mater. Technol.* **2022**, *31*, e00369.
[124] a) Y. Wang, S. Zhang, J. Wang, *Chin. Chem. Lett.* **2021**, *32*, 1603; b) H. Ma, Y. Peng, S. Zhang, Y. Zhang, P. Min, *Gels* **2022**, *8*, 609.
[125] a) A. Ashfaq, M.-C. Clochard, X. Coqueret, C. Dispenza, M. S. Driscoll, P. Ulański, M. Al-Sheikhly, *Polymers* **2020**, *12*, 2877; b) R. Blažic, K. Marušić, E. Vidović, *Gels* **2023**, *9*, 94.
[126] B. Yao, S. Wu, R. Wang, Y. Yan, A. Cardenas, D. Wu, Y. Alsaid, W. Wu, X. Zhu, X. He, *Adv. Funct. Mater.* **2022**, *32*, 2109506.
[127] a) K. M. Lee, Y. Oh, H. Yoon, M. Chang, H. Kim, *ACS Appl. Mater. Interfaces* **2020**, *12*, 8642; b) A. Roy, P. P. Maity, S. Dhara, S. Pal, *J. Appl. Polym. Sci.* **2018**, *135*, 45939; c) S. A. Ghumman, S. Noreen, H. Hameed, M. A. Elsherif, R. Shabbir, M. Rana, K. Junaid, S. N. A. Bukhari, *Gels* **2022**, *8*, 291.
[128] Y. Wang, X. Wang, Y. Xie, K. Zhang, *Cellulose* **2018**, *25*, 3703.
[129] A. Hufendiek, C. Barner-Kowollik, M. A. Meier, *Polym. Chem.* **2015**, *6*, 2188.
[130] S. Chu, M. M. Maples, S. J. Bryant, *Acta Biomater.* **2020**, *109*, 37.
[131] E. Badali, M. Hosseini, M. Mohajer, S. Hassanzadeh, S. Saghati, J. Hilborn, M. Khanmohammadi, *Polym. Sci., Ser. A* **2021**, *63*, S1.
[132] N. T. Phuong, V. Anh Ho, D. Hai Nguyen, N. C. Khoa, T. N. Quyen, Y. Lee, K. D. Park, *J. Bioact. Compat. Polym.* **2015**, *30*, 412.
[133] P. Sapuła, K. Bialik-Wąs, K. Malarz, *Pharmaceutics* **2023**, *15*, 253.
[134] a) A. Sionkowska, M. Michalska-Sionkowska, M. Walczak, *Int. J. Biol. Macromol.* **2020**, *149*, 290; b) Z. Xu, L. Yuan, Q. Liu, D. Li, C. Mu, L. Zhao, X. Li, L. Ge, *Carbohydr. Polym.* **2022**, *285*, 119237.
[135] a) L. S. F. Leite, C. Pham, S. Bilatto, H. M. Azeredo, E. D. Cranston, F. K. Moreira, L. H. C. Mattoso, J. Bras, *ACS Sustainable Chem. Eng.* **2021**, *9*, 8539; b) W. Ge, S. Cao, F. Shen, Y. Wang, J. Ren, X. Wang, *Carbohydr. Polym.* **2019**, *224*, 115147.
[136] a) B. Manickam, R. Sreedharan, M. Elumalai, *Curr. Drug Delivery* **2014**, *11*, 139; b) S. I. Erdagi, F. A. Ngwabebhoh, U. Yildiz, *Int. J. Biol. Macromol.* **2020**, *149*, 651.
[137] A.-L. Oechsle, L. Lewis, W. Y. Hamad, S. G. Hatzikiriakos, M. J. MacLachlan, *Chem. Mater.* **2018**, *30*, 376.
[138] P. Li, Z. Ling, X. Liu, L. Bai, W. Wang, H. Chen, H. Yang, L. Yang, D. Wei, *Chem. Eng. J.* **2023**, *466*, 143306.
[139] H. Wang, Z. Li, M. Zuo, X. Zeng, X. Tang, Y. Sun, L. Lin, *Carbohydr. Polym.* **2022**, *280*, 119018.
[140] X. Liu, X. He, B. Yang, L. Lai, N. Chen, J. Hu, Q. Lu, *Adv. Funct. Mater.* **2021**, *31*, 2008187.
[141] Y. Wang, Q. Wang, S. Liu, X. Ji, G. Yang, J. Chen, *Carbohydr. Polym.* **2022**, *284*, 119193.
[142] R. Tong, G. Chen, D. Pan, H. Qi, R. a. Li, J. Tian, F. Lu, M. He, *Biomacromolecules* **2019**, *20*, 2096.
[143] Y. Zhong, J. Wang, Z. Yuan, Y. Wang, Z. Xi, L. Li, Z. Liu, X. Guo, *Colloids Surf., B* **2019**, *179*, 462.
[144] Y. Ko, D. Kim, U.-J. Kim, J. You, *Carbohydr. Polym.* **2017**, *173*, 383.
[145] X. Du, Z. Zhang, W. Liu, Y. Deng, *Nano Energy* **2017**, *35*, 299.
[146] T. Kasuga, T. Saito, H. Koga, M. Nogi, *ACS Nano* **2022**, *16*, 18390.
[147] J. Luo, T. Song, T. Han, H. Qi, Q. Liu, T. Rosenau, *Chem. Eng. J.* **2024**, *493*, 152649.
[148] a) C. Meng, C. Liu, L. Chen, C. Hu, S. Fan, *Nano Lett.* **2010**, *10*, 4025; b) H. Wang, J. Lin, Z. X. Shen, *J. Sci.: Adv. Mater. Devices* **2016**, *1*, 225; c) W. A. Marmisollé, M. I. Florit, D. Posadas, *J. Electroanal. Chem.* **2012**, *673*, 65.
[149] G. Soukupová, T. Bautkinová, P. Mazúr, J. Vilčáková, J. Prokeš, M. Dendisová, M. Lhotka, F. Hassouna, *Electrochim. Acta* **2023**, *441*, 141830.
[150] R. Brooke, M. Lay, K. Jain, H. Francon, M. G. Say, D. Belaineh, X. Wang, K. M. Håkansson, L. Wågberg, I. Engquist, *Polym. Rev.* **2023**, *63*, 437.
[151] T.-C. Wei, S.-H. Chen, C.-Y. Chen, *Mater. Chem. Front.* **2020**, *4*, 3302.
[152] a) P. M. Inácio, M. C. Medeiros, T. Carvalho, R. C. Felix, A. Mestre, P. C. Hubbard, Q. Ferreira, J. Morgado, A. Charas, C. S. Freire, *Org. Electron.* **2020**, *85*, 105882; b) C. Chen, T. Zhang, Q. Zhang, Z. Feng, C. Zhu, Y. Yu, K. Li, M. Zhao, J. Yang, J. Liu, *ACS Appl. Mater. Interfaces* **2015**, *7*, 28244.
[153] C. Chen, X. Chen, H. Zhang, Q. Zhang, L. Wang, C. Li, B. Dai, J. Yang, J. Liu, D. Sun, *Acta Biomater.* **2017**, *55*, 434.
[154] Y. Liu, D. Jiang, Z. Wu, B. Jiang, Q. Xu, *Sens. Actuators, A* **2024**, *370*, 115258.
[155] a) C. Sang, S. Wang, X. Jin, X. Cheng, H. Xiao, Y. Yue, J. Han, *Carbohydr. Polym.* **2024**, *333*, 121947; b) Y. Lu, Y. Yue, Q. Ding, C. Mei, X. Xu, Q. Wu, H. Xiao, J. Han, *ACS Appl. Mater. Interfaces* **2021**, *13*, 50281.
[156] A. Rudich, S. Sapru, O. Shoseyov, *Nanomaterials* **2023**, *13*, 853.
[157] Y. Lu, Y. Yue, Q. Ding, C. Mei, X. Xu, S. Jiang, S. He, Q. Wu, H. Xiao, J. Han, *InfoMat* **2023**, *5*, e12409.
[158] F. Amir, M. B. K. Niazi, U. S. Malik, Z. Jahan, S. Andleeb, T. Ahmad, Z. Mustansar, *Int. J. Biol. Macromol.* **2024**, *258*, 128831.
[159] Y. Li, Q. Gong, X. Liu, Z. Xia, Y. Yang, C. Chen, C. Qian, *Carbohydr. Polym.* **2021**, *267*, 118207.
[160] X. Fu, J. K. Wang, A. C. Ramírez-Pérez, C. Choong, G. Lisak, *Mater. Sci. Eng., C* **2020**, *108*, 110392.
[161] Z. Wang, Z. Ma, S. Wang, M. Pi, X. Wang, M. Li, H. Lu, W. Cui, R. Ran, *Carbohydr. Polym.* **2022**, *298*, 120128.
[162] Y. Nie, D. Yue, W. Xiao, W. Wang, H. Chen, L. Bai, L. Yang, H. Yang, D. Wei, *Chem. Eng. J.* **2022**, *436*, 135243.
[163] Z. Chen, Y. Hu, G. Shi, H. Zhuo, M. A. Ali, E. Jamróz, H. Zhang, L. Zhong, X. Peng, *Adv. Funct. Mater.* **2023**, *33*, 2214245.
[164] A. Khalid, A. Madni, B. Raza, M. ul Islam, A. Hassan, F. Ahmad, H. Ali, T. Khan, F. Wahid, *Int. J. Biol. Macromol.* **2022**, *203*, 256.

[165] U. D'Amora, S. Dacrory, M. S. Hasanin, A. Longo, A. Soriente, S. Kamel, M. G. Raucci, L. Ambrosio, S. Scialla, *Pharmaceutics* **2023**, *15*, 338.
[166] G. Xiao, Y. Wang, H. Zhang, Z. Zhu, S. Fu, *Int. J. Biol. Macromol.* **2021**, *170*, 272.
[167] P. Wei, L. Wang, F. Xie, J. Cai, *Chem. Eng. J.* **2022**, *431*, 133964.
[168] L. Zhao, Z. Ren, X. Liu, Q. Ling, Z. Li, H. Gu, *ACS Appl. Mater. Interfaces* **2021**, *13*, 11344.
[169] T. Chen, T. Yao, H. Peng, A. K. Whittaker, Y. Li, S. Zhu, Z. Wang, *Adv. Funct. Mater.* **2021**, *31*, 2106079.
[170] a) S. Panda, K. Deshmukh, S. K. Pasha, J. Theerthagiri, S. Manickam, M. Y. Choi, *Coord. Chem. Rev.* **2022**, *462*, 214518; b) K. Nasrin, V. Sudharshan, K. Subramani, M. Sathish, *Adv. Funct. Mater.* **2022**, *32*, 2110267.
[171] a) Y. Zhang, Z. Xu, Y. Yuan, C. Liu, M. Zhang, L. Zhang, P. Wan, *Adv. Funct. Mater.* **2023**, *33*, 2300299; b) W. Zhang, P.-L. Wang, L.-Z. Huang, W.-Y. Guo, J. Zhao, M.-G. Ma, *Nano Energy* **2023**, *117*, 108875; c) H. Wan, Y. Chen, Y. Tao, P. Chen, S. Wang, X. Jiang, A. Lu, *ACS Nano* **2023**, *17*, 20699.
[172] B. Wan, N. Liu, Z. Zhang, X. Fang, Y. Ding, H. Xiang, Y. He, M. Liu, X. Lin, J. Tang, *Carbohydr. Polym.* **2023**, *314*, 120929.
[173] X. Nie, Y. Xie, X. Ding, L. Dai, F. Gao, W. Song, X. Li, P. Liu, Z. Tan, H. Shi, *Carbohydr. Polym.* **2024**, *334*, 122068.
[174] P. He, R. Guo, K. Hu, K. Liu, S. Lin, H. Wu, L. Huang, L. Chen, Y. Ni, *Chem. Eng. J.* **2021**, *414*, 128726.
[175] R. Li, K. Liu, X. Huang, D. Li, J. Ding, B. Liu, X. Chen, *Adv. Sci.* **2022**, *9*, 2105152.
[176] X. Zhao, H. Wu, B. Guo, R. Dong, Y. Qiu, P. X. Ma, *Biomaterials* **2017**, *122*, 34.
[177] a) Y. Liang, J. He, B. Guo, *ACS Nano* **2021**, *15*, 12687; b) R. Luo, Y. Liang, J. Yang, H. Feng, Y. Chen, X. Jiang, Z. Zhang, J. Liu, Y. Bai, J. Xue, *Adv. Mater.* **2023**, *35*, 2208395.
[178] M. Talikowska, X. Fu, G. Lisak, *Biosens. Bioelectron.* **2019**, *135*, 50.
[179] a) H. Lei, D. Fan, *Chem. Eng. J.* **2021**, *421*, 129578; b) K. Han, Q. Bai, W. Wu, N. Sun, N. Cui, T. Lu, *Int. J. Biol. Macromol.* **2021**, *183*, 2142.
[180] L. Wang, T. Xu, X. Zhang, *TrAC, Trends Anal. Chem.* **2021**, *134*, 116130.
[181] a) F. Chen, M. Wu, Q. Dong, M. Ke, X. Liang, J. Ai, Q. Cheng, L. Cai, Z. Tong, Y. Chen, *Composites, Part B* **2022**, *238*, 109903; b) N. Nguyen, Z.-H. Lin, S. R. Barman, C. Korupalli, J.-Y. Cheng, N.-X. Song, Y. Chang, F.-L. Mi, H.-L. Song, H.-W. Sung, *Nano Energy* **2022**, *99*, 107393.
[182] a) C. Frantz, K. M. Stewart, V. M. Weaver, *J. Cell Sci.* **2010**, *123*, 4195; b) A. D. Theocharis, S. S. Skandalis, C. Gialeli, N. K. Karamanos, *Adv. Drug Delivery Rev.* **2016**, *97*, 4.
[183] K. A. McLaughlin, M. Levin, *Dev. Biol.* **2018**, *433*, 177.
[184] a) C. Chen, X. Bai, Y. Ding, I.-S. Lee, *Biomater. Res.* **2019**, *23*, 25; b) J. Du, G. Zhen, H. Chen, S. Zhang, L. Qing, X. Yang, G. Lee, H.-Q. Mao, X. Jia, *Biomaterials* **2018**, *181*, 347.
[185] a) M. T. Spang, K. L. Christman, *Acta Biomater.* **2018**, *68*, 1; b) A. D. Rape, M. Zibinsky, N. Murthy, S. Kumar, *Nat. Commun.* **2015**, *6*, 8129; c) P. Slivka, C. Dearth, T. Keane, F. Meng, C. Medberry, R. Riggio, J. Reing, S. Badylak, *Biomater. Sci.* **2014**, *2*, 1521.
[186] Y. Li, H. Zhang, S. Ni, H. Xiao, *Mater. Lett.* **2018**, *232*, 175.
[187] Y. J. Cheah, M. H. M. Yunus, M. B. Fauzi, Y. Tabata, Y. Hiraoka, S. J. Phang, M. R. Chia, M. R. Buyong, M. D. Yazid, *Cellulose* **2023**, *30*, 5071.
[188] M. Ghorbani, L. Roshangar, J. S. Rad, *Eur. Polym. J.* **2020**, *130*, 109697.
[189] X.-y. Zhang, Y.-p. Chen, J. Han, J. Mo, P.-f. Dong, Y.-h. Zhuo, Y. Feng, *Int. J. Biol. Macromol.* **2019**, *136*, 1247.
[190] J. Han, Q. Ding, C. Mei, Q. Wu, Y. Yue, X. Xu, *Electrochim. Acta* **2019**, *318*, 660.
[191] M. Bordoni, E. Karabulut, V. Kuzmenko, V. Fantini, O. Pansarasa, C. Cereda, P. Gatenholm, *Cells* **2020**, *9*, 682.
[192] L. Wang, S. Hu, M. W. Ullah, X. Li, Z. Shi, G. Yang, *Carbohydr. Polym.* **2020**, *249*, 116829.
[193] H. Tohidi, N. Maleki-Jirsaraei, A. Simchi, F. Mohandes, Z. Emami, L. Fassina, F. Naro, B. Conti, F. Barbagallo, *Materials* **2022**, *15*, 5122.
[194] S. Y. Srinivasan, M. Cler, O. Zapata-Arteaga, B. Dörling, M. Campoy-Quiles, E. Martínez, E. Engel, S. Pérez-Amodio, A. Laromaine, *ACS Appl. Bio Mater.* **2023**, *6*, 2860.
[195] S. Khan, M. Ul-Islam, M. W. Ullah, M. Israr, J. H. Jang, J. K. Park, *Int. J. Biol. Macromol.* **2018**, *107*, 865.
[196] D. Aki, S. Ulag, S. Unal, M. Sengor, N. Ekren, C.-C. Lin, H. Yılmazer, C. B. Ustundag, D. M. Kalaskar, O. Gunduz, *Mater. Des.* **2020**, *196*, 109094.
[197] C. C. Hornat, M. W. Urban, *Prog. Polym. Sci.* **2020**, *102*, 101208.
[198] A. Shaabani, R. Sedghi, H. Motasadizadeh, R. Dinarvand, *Chem. Eng. J.* **2021**, *411*, 128449.
[199] C. Chen, Z. Hou, S. Chen, J. Guo, Z. Chen, J. Hu, L. Yang, *Composites, Part B* **2022**, *240*, 109985.
[200] R. Nasseri, N. Bouzari, J. Huang, H. Golzar, S. Jankhani, X. Tang, T. H. Mekonnen, A. Aghakhani, H. Shahsavan, *Nat. Commun.* **2023**, *14*, 6108.
[201] R. Goyal, S. Sahu, S. Mitra, R. Niranjan, R. Priyadarshini, R. Yadav, B. Lochab, *ACS Appl. Polym. Mater* **2024**, *6*, 1348.
[202] X. Zhang, Y. Wang, J. Zhao, M. Xiao, W. Zhang, C. Lu, *ACS Sustainable Chem. Eng.* **2016**, *4*, 4321.
[203] Z. Jiang, Y. Wang, Z. Huang, W. Ma, S. Gao, W. Dong, M. Xu, *Carbohydr. Polym.* **2022**, *276*, 118767.
[204] a) X. Jiang, X. Yang, B. Yang, L. Zhang, A. Lu, *Carbohydr. Polym.* **2021**, *273*, 118547; b) Y. Wang, Y. Wu, L. Long, L. Yang, D. Fu, C. Hu, Q. Kong, Y. Wang, *ACS Appl. Mater. Interfaces* **2021**, *13*, 33584; c) Y. Hu, J. Y. Ying, *Mater. Today* **2023**, *63*, 188.
[205] S. Cho, S. Y. Hwang, D. X. Oh, J. Park, *J. Mater. Chem. A* **2021**, *9*, 14630.
[206] a) Y. Wu, Y. Li, R. Han, Z. Long, P. Si, D. Zhang, *Biomacromolecules* **2023**, *24*, 5364; b) S. Xue, G. Liu, J. Lai, P. An, Y. Liu, Y. Wu, Y. Wang, Z. Ye, Q. Tang, H. Zhou, *Macromol. Mater. Eng.* **2021**, *306*, 2100415.
[207] M. Li, S. Fu, A. H. Basta, *Carbohydr. Polym.* **2020**, *230*, 115676.
[208] H. Zhang, Y. Zhao, *ACS Appl. Mater. Interfaces* **2013**, *5*, 13069.
[209] M. Li, S. Fu, L. A. Lucia, Y. Wang, *Compos. Sci. Technol.* **2020**, *199*, 108371.
[210] Y. Ma, Y. Lu, Y. Yue, S. He, S. Jiang, C. Mei, X. Xu, Q. Wu, H. Xiao, J. Han, *Carbohydr. Polym.* **2024**, *335*, 122067.
[211] G. Xiao, S. Fu, L. A. Lucia, *Carbohydr. Polym.* **2021**, *255*, 117495.
[212] A. Toncheva, F. Khelifa, Y. Paint, M. Voué, P. Lambert, P. Dubois, J.-M. Raquez, *ACS Appl. Mater. Interfaces* **2018**, *10*, 29933.
[213] a) H.-M. Zhang, Y.-P. Wang, S.-F. Zhang, W.-B. Niu, *ACS Appl. Mater. Interfaces* **2022**, *14*, 54936; b) H. Zhang, J. Guo, Y. Wang, L. Sun, Y. Zhao, *Adv. Sci.* **2021**, *8*, 2102156.
[214] L. Sun, Z. Chen, D. Xu, Y. Zhao, *Adv. Sci.* **2022**, *9*, 2105777.
[215] Y. Wang, J. Guo, L. Sun, H. Chen, Y. Zhao, *Chem. Eng. J.* **2021**, *415*, 128978.
[216] C. Xu, C. Huang, H. Huang, *Appl. Mater. Today* **2021**, *22*, 100912.
[217] Z.-L. Zhang, X. Dong, Y.-Y. Zhao, F. Song, X.-L. Wang, Y.-Z. Wang, *Biomacromolecules* **2022**, *23*, 4110.
[218] A. Babaei-Ghazvini, B. Acharya, *Chem. Eng. J.* **2023**, *476*, 146585.
[219] J. P. Lagerwall, C. Schütz, M. Salajkova, J. Noh, J. Hyun Park, G. Scalia, L. Bergström, *NPG Asia Mater.* **2014**, *6*, e80.
[220] X. Li, Y. Yang, C. Valenzuela, X. Zhang, P. Xue, Y. Liu, C. Liu, L. Wang, *ACS Nano* **2023**, *17*, 12829.
[221] L. Huang, X. Zhang, L. Deng, Y. Wang, Y. Liu, H. Zhu, *ACS Nano* **2024**, *18*, 3627.
[222] J. Wei, X. Aeby, G. Nyström, *Adv. Mater. Technol.* **2023**, *8*, 2200897.

[223] Z. Liu, X. Chen, Z. L. Wang, *Adv. Mater.* **2024**, *2024*, 2409440.
[224] a) Z. Niu, W. Cheng, M. Cao, D. Wang, Q. Wang, J. Han, Y. Long, G. Han, *Nano Energy* **2021**, *87*, 106175; b) S. Fang, X. Ji, H. Wang, H. Jiang, M. Gao, H. Liu, Y. Liu, B. Cheng, *J. Mater. Chem. A* **2024**, *12*, 9322.
[225] Z. Jin, F. Zhao, Y. Lei, Y.-C. Wang, *Nano Energy* **2022**, *95*, 106988.
[226] Y. Zhou, G. Huang, Z. Zhang, L. Qin, H. Cai, J. Sha, *ACS Appl. Nano Mater.* **2024**, *7*.
[227] a) R. Yao, X. Liu, H. Yu, Z. Hou, S. Chang, L. Yang, *Int. J. Biol. Macromol.* **2024**, *278*, 134694; b) S. H. D. Wong, G. R. Deen, J. S. Bates, C. Maiti, C. Y. K. Lam, A. Pachauri, R. AlAnsari, P. Bělský, J. Yoon, J. M. Dodda, *Adv. Funct. Mater.* **2023**, *33*, 2213560.
[228] a) Y. Lu, Y. Chen, H. Sun, F. Deng, C. Mei, X. Xu, Q. Wu, H. Xiao, Y. Yue, J. Han, *npj Flexible Electron.* **2024**, *8*, 37; b) Y. Lu, H. Sun, F. Deng, Y. Yue, S. He, S. Jiang, Q. Wu, H. Xiao, J. Han, *ACS Sustainable Chem. Eng.* **2024**, *12*, 7976.
[229] W. Chen, J. Ma, D. Yu, N. Li, X. Ji, *Int. J. Biol. Macromol.* **2024**, *266*, 131129.
[230] X. Yan, X. Lin, H. Liu, J. Lu, H. Wang, X. Huang, H. Liu, X. Xu, *Carbohydr. Polym.* **2024**, *344*, 122552.
[231] H. Sun, Y. Lu, Y. Chen, Y. Yue, S. Jiang, X. Xu, C. Mei, H. Xiao, J. Han, *Carbohydr. Polym.* **2022**, *296*, 119891.
[232] a) Y. Yue, X. Wang, J. Han, L. Yu, J. Chen, Q. Wu, J. Jiang, *Carbohydr. Polym.* **2019**, *206*, 289; b) N. Lin, A. Gèze, D. Wouessidjewe, J. Huang, A. Dufresne, *ACS Appl. Mater. Interfaces* **2016**, *8*, 6880.
[233] V. G. Phan, M. Murugesan, H. Huong, T.-T. Le, T.-H. Phan, P. Manivasagan, R. Mathiyalagan, E.-S. Jang, D. C. Yang, Y. Li, *ACS Appl. Mater. Interfaces* **2022**, *14*, 42812.
[234] S. Wang, X. Jin, Y. Yue, C. Mei, X. Xu, Q. Wu, H. Xiao, J. Han, *Chem. Eng. J.* **2023**, *470*, 144225.
[235] Q. Yang, M. He, Z. Yu, Y. Liu, Y. Bai, T. Liu, T. Wang, L. Meng, F. Meng, Q. Ma, Y. Che, *Chem. Eng. J.* **2024**, *495*, 153567.
[236] L. Han, S. Cui, H.-Y. Yu, M. Song, H. Zhang, N. Grishkewich, C. Huang, D. Kim, K. M. C. Tam, *ACS Appl. Mater. Interfaces* **2019**, *11*, 44642.
[237] M. Song, H. Yu, J. Zhu, Z. Ouyang, S. Y. H. Abdalkarim, K. C. Tam, Y. Li, *Chem. Eng. J.* **2020**, *398*, 125547.
[238] a) Y. Wang, L. Chen, *Carbohydr. Polym.* **2011**, *83*, 1937; b) D. Haldar, M. K. Purkait, *Carbohydr. Polym.* **2020**, *250*, 116937.
[239] T. Chen, Y. Yang, H. Peng, A. K. Whittaker, Y. Li, Q. Zhao, Y. Wang, S. Zhu, Z. Wang, *Carbohydr. Polym.* **2021**, *266*, 118122.
[240] S. Jacob, S. Antony, A. Madhavan, R. Sindhu, M. Kumar Awasthi, M. Kuddus, S. Pillai, S. Varjani, A. Pandey, P. Binod, *Bioengineered* **2022**, *13*, 12823.
[241] Q. Ding, X. Xu, Y. Yue, C. Mei, C. Huang, S. Jiang, Q. Wu, J. Han, *ACS Appl. Mater. Interfaces* **2018**, *10*, 27987.

**Myoung Joon Jeon** is a master's student in Biosystems Engineering at Kangwon National University, South Korea. His research interest is nanocellulose-based 3D printed hydrogel for sensing and wound healing.

**Aayushi Randhawa** is a doctoral student in Biosystems Engineering at Kangwon National University, South Korea. She received her Master's degree from Bangalore University, India. Her research interest is developing stimuli-dependent regenerative therapies for healing damaged tissues.

**Hojin Kim** is a master's student in Biosystems Engineering at Kangwon National University, South Korea. His research interest is nanocellulose hydrogel for multifunctional sensing.

**Sayan Deb Dutta** is a postdoctoral research associate at Kangwon National University. He received his doctoral degree from the Department of Biosystems Engineering at Kangwon National University, South Korea. He received his Master's degree from the University of Kalyani, India. His research interest is the synthesis of multifunctional nanomaterials for 3D printing and nanotheranostic applications for tissue engineering and biosensing.

**Keya Ganguly** is a Postdoctoral Research Associate at Kangwon National University. She received her doctoral degree from the Department of Biosystems Engineering at Kangwon National University, South Korea. She received her Master's degree from Presidency University, India. Her research interest is developing a multistimuli-assisted scaffolding platform for tissue engineering and biosensing.

**Tejal V. Patil** is a doctoral student of Biosystems Engineering at Kangwon National University, South Korea. She received her Master's degree from the Institute of Chemical Technology, Mumbai, India. Her research interest is developing biomaterials for application in bacteria eradication and tissue regeneration.

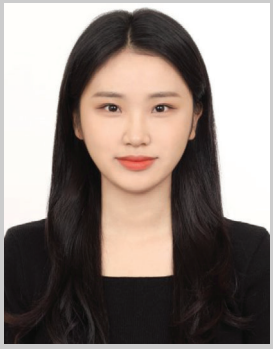

**Jieun Lee** is a master's student in Biosystems Engineering at Kangwon National University, South Korea. Her research is the development of various conductive 3D hydrogels for tissue regeneration and healing.

**Rumi Acharya** is a doctoral student in Biosystems Engineering at Kangwon National University, South Korea. She received her master's degree from Guru Ghasidas University, India. Her research interests are Nano biosensors and magnetogenetic therapy on cellular targets.

**Hyeonseo Park** is a master's student in Biosystems Engineering at Kangwon National University, South Korea. Her research interest is guided wound healing using nanofiber scaffolds through an electrospinning technique.

**Youjin Seol** is a master's student in Biosystems Engineering at Kangwon National University, South Korea. Her research interest is the development of bioinspired nanoparticle-containing 3D hydrogels for wound healing and biosensing.

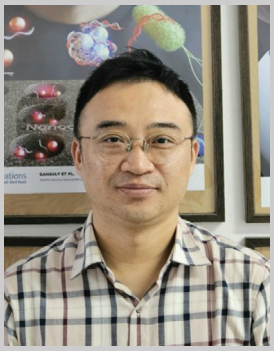

**Ki-Taek Lim** is a professor at the Department of Biosystems Engineering at Kangwon National University, South Korea. He received his doctoral degree from Seoul National University, South Korea, and joined as a postdoctoral research fellow at the University of Arkansas, USA. He has a strong knowledge of mechatronics and regenerative medicines. His research focuses on developing the bio-nanorobotics system with novel bioreactors and stem cell cultures for tissue-engineering applications.